UNIVERZITA KARLOVA V PRAZE
Přírodovědecká fakulta

Studijní program: Chemie
Studijní obor: Chemie v přírodních vědách

Miriam Basová

Soli heteroaromatických sloučenin pro NLO
Salts of Heteroaromatic Compounds for NLO

Katedra anorganické chemie

Bakalářská práce

Vedoucí bakalářské práce: Doc. RNDr. Ivan Němec, Ph.D.
Konzultant: RNDr. Irena Matulková, Ph.D.

Praha 2015

CHARLES UNIVERSITY IN PRAGUE
Faculty of Science

Study programme: Chemistry
Study course: Chemistry in Natural Science

Miriam Basová

Soli heteroaromatických sloučenin pro NLO
Salts of Heteroaromatic Compounds for NLO

Department of Inorganic Chemistry

Bachelor's thesis

Supervisor: Doc. RNDr. Ivan Němec, Ph.D.
Consultant: RNDr. Irena Matulková, Ph.D.

Prague 2015

Tato práce vznikla v souvislosti s řešením grantu GAČR 14 – 05506S.

Prohlášení

Prohlašuji, že jsem tuto závěrečnou práci zpracovala samostatně pod vedením školitele doc. RNDr. Ivana Němce, Ph.D. a RNDr. Ireny Matulkové, Ph.D. a že jsem uvedla všechny použité informační zdroje a literaturu. Tato práce ani její podstatná část nebyla předložena k získání jiného nebo stejného akademického titulu.

Jsem si vědomá toho, že případné využití výsledků, získaných v této práci, mimo Univerzitu Karlovu v Praze je možné pouze po písemném souhlasu této Univerzity.

V Praze dne 15. srpna 2015 Miriam Basová

This thesis was supported by Czech Science Foundation by grant No. 14 – 05506S.

Declaration

I declare that I prepared this bachelor's thesis individually under supervision of doc. RNDr. Ivan Němec, Ph.D. and RNDr. Irena Matulková, Ph.D. and that I cited all used information and literature sources properly. Neither this thesis nor its significant part has been previously submitted for obtaining any academic degree.

I am aware that the results obtained in this work can be used outside the Charles University in Prague only with the written consent of this University.

Prague, August 15th, 2015. Miriam Basová

Acknowledgements

I would like to express my gratitude to my supervisor doc. RNDr. Ivan Němec, Ph.D. for his professional support, kind help and priceless patience during the work on this thesis. My gratitude also includes RNDr. Irena Matulková, Ph.D. for her wise advice and kind help, RNDr. Ivana Císařová, CSc. for determination of single crystal structures, Martina Malíková for measuring the powder X-ray diffraction data and doc. RNDr. Petr Němec, CSc. from Faculty of Mathematics and Physics, Department of Chemical Physics and Optics for SHG measurements and brief explanation of SHG theory.

Last but not least I would like to thank my colleagues from laboratory for friendly atmosphere and my family and friends for their priceless support during whole my study.

Abstrakt

Předkládaná bakalářská práce je zaměřena na přípravu a studium sloučenin 2,4-diamino-1,3,5-triazinu. Primárním cílem bylo připravit a charakterizovat soli nebo adukty 2,4-diamino-1,3,5-triazinu s vybranými anorganickými a organickými kyselinami, přičemž pozornost byla zaměřena zejména na jejich využití jako nových materiálů pro nelineární optiku. Připravené materiály byly charakterizovány především pomocí metod infračervené a Ramanovy spektroskopie a RTG difrakce. Pro interpretaci vibračních spekter a odhad nelineárních optických vlastností vybraných molekul byly využity kvantově-chemické výpočty. Na závěr byla u sloučenin s necentrosymetrickým uspořádáním studována účinnost generování druhé harmonické frekvence na práškových vzorcích.

Abstract

The main target of this bachelor's thesis is the preparation and characterization of novel compounds with expected non-linear optical properties. Starting material for the preparation of new salts was 2,4-diamino-1,3,5-triazine. These salts or co-crystals were prepared by the crystallization with selected inorganic and organic acids. The methods of infrared and Raman spectroscopy along with X-ray diffraction methods were used to characterize the prepared materials. Moreover, the NLO potential of selected molecules was proven by quantum – chemical calculations. These calculations were also used for the interpretation of the vibrational spectra. Finally, the structures with non-centrosymmetric assembly were examined for the second harmonic generation efficiency in powdered samples.

Klíčová slova: nelineární optika, 2,4-diamino-1,3,5-triazin, vibrační spektroskopie, strukturní analýza

Keywords: non-linear optics, 2,4-diamino-1,3,5-triazine, vibrational spectroscopy, structural analysis

1 Contents

2 Abbreviations

SHG	second harmonic generation
NLO	non-linear optics
KDP	potassium dihydrogen phosphate
SCF	self-consistent field
B3LYP	Becke-3-Lee-Yang-Parr
DAMT	2,4-diamino-1,3,5-triazine
DAMT NO_3	2,4-diamino-1,3,5-triazinium(1+) nitrate
$(DAMT)_2\ SO_4 \cdot H_2O$	bis(2,4-diamino-1,3,5-triazinium(1+)) sulfate monohydrate
DAMT H_2PO_3	2,4-diamino-1,3,5-triazinium(1+) hydrogen phosphite
DAMT H_2PO_4	2,4-diamino-1,3,5-triazinium(1+) dihydrogen phosphate
$(DAMT)_2\ ClO_4 \cdot 2H_2O$	2,4-diamino-1,3,5-triazine 2,4-diamino-1,3,5-triazinium(1+) perchlorate dihydrate
DAMT Cl	2,4-diamino-1,3,5-triazinium(1+) chloride
DAMT Hmalon	2,4-diamino-1,3,5-triazinium(1+) hydrogen malonate
DAMT $H_2suc \cdot H_2O$	2,4-diamino-1,3,5-triazine – succinic acid (1/1) monohydrate
DAMT Hsuc	2,4-diamino-1,3,5-triazinium(1+) hydrogen succinate
DAMT H_2glu	2,4-diamino-1,3,5-triazine – glutaric acid (1/1)
DAMT H_2adp	2,4-diamino-1,3,5-triazine – adipic acid (1/1)
DAMT HLmal $\cdot H_2O$	2,4-diamino-1,3,5-triazinium(1+) hydrogen L–malate monohydrate
$(DAMT)_2$ Ltar	bis(2,4-diamino-1,3,5-triazinium(1+)) L–tartrate

Symbols in equations:

μ	dipole moment
N	number density of dipole moment
α	linear polarizability
β	hyperpolarizability
E	electric field intensity
P	induced dielectric polarization
χ	dielectric susceptibility tensor
ω	angular frequency

Symbols used for vibrational spectra assignment:

s	strong
m	medium
w	weak
ν_s	symmetric stretching vibration
ν_{as}	anti-symmetric stretching vibration
δ	deformation or in-plane bending vibration
γ	out-of-plane bending vibration
ρ	rocking vibration
ω	wagging vibration
τ	twisting vibration
RG	vibration of aromatic ring
sci	scissoring vibration

3 Theoretical part

3.1 Non-linear optics

Chemistry of crystalline materials with non-linear optical properties is one of the most attractive fields of current scientific research. The motivation for this interest is mainly a large number of applications such as area of optical modulation, optical switching, frequency shifting and optical data storage for the development and improvement of technologies in telecommunications and signal processing.[1, 2, 3]

A non-linear dielectric medium is characterized by a non-linear relation between the induced dielectric polarization $\boldsymbol{P}$ and the applied field $\boldsymbol{E}$. The non-linearity may be of macroscopic and microscopic origin. The polarization density $\boldsymbol{P} = N\boldsymbol{\mu}$ is a product of the individual dipole moment $\boldsymbol{\mu}$ induced by the applied electric field $\boldsymbol{E}$ and the number density of dipole moments N. The non-linear behavior may reside either in $\boldsymbol{P}$ or in N.[4]

The relation between $\boldsymbol{P}$ and $\boldsymbol{E}$ is linear when $\boldsymbol{E}$ is very small but becomes non-linear when $\boldsymbol{E}$ acquires values comparable to interatomic electric fields which are typically $\sim 10^5 - 10^8$ V/m.[4] The induced dielectric polarization dependence on the applied field can be expressed by the Equation 1

$$\boldsymbol{P}(\boldsymbol{E}) = \varepsilon_0 (\chi^{(1)} \boldsymbol{E}^1 + \chi^{(2)} \boldsymbol{E}^2 + \chi^{(3)} \boldsymbol{E}^3 + \ldots) \quad (1)$$

where $\chi^{(1)}$ is the linear dielectric susceptibility pertinent to linear optics and $\chi^{(2)}$, $\chi^{(3)}$, … are the non-linear susceptibilities of the second, third and higher orders, respectively. The χ coefficients are crucial for the non-linear optical properties as the non-linear phenomenon occurs when the polarization of the material responds non-linearly to the interaction with the electric component of the light.

3.2 Second harmonic generation

Second harmonic generation, often called frequency doubling, belongs to the second order non-linear optical phenomena. It is a special case of sum frequency generation in which photons with the same frequency ω are destroyed to create a single photon with frequency of 2ω.[1] The main condition for SHG to be observed is the non-centrosymmetric assembly of the compounds because only here a non-zero second order non-linear susceptibility can occur.

For generating sum frequency ω_3 in material from the frequencies ω_1 and ω_2 it is requested not only that $\omega_3 = \omega_1 + \omega_2$ but also $\boldsymbol{k_3} = \boldsymbol{k_1} + \boldsymbol{k_2}$ which means that all three waves are in phase and it is important for the maximum intensity of their interaction. For SHG this

phase matching condition is $\boldsymbol{k_2} = 2\boldsymbol{k_1}$ for the incident radiation wave and the generated wave to be in phase.[1]

The efficiency of the SHG generation depends on the refractive indices and phase matchability and on the quality and the orientation of the crystal.

3.3 Materials for SHG

Previously studied and characterized materials for SHG can be divided to three main groups: 1. inorganic salts and oxides, 2. organic and inorganic molecules and 3. organic salts and co-crystals.[5]

The materials such as ADP ($NH_4H_2PO_4$) and KDP (KH_2PO_4), BBO (β-BaB_2O_4), $LiNbO_3$ belong to the first group. Their advantages are mainly the high melting points, hardness and a relative wide transparency window in the Vis and UV region.[1, 5] On the other hand, disadvantages of these materials are limited transparency in IR region, low non-linear coefficients and low resistivity to the optical damage.

Materials from the second group are studied because of their high values of hyperpolarizability β, high resistivity to the optical damage, possibility to modify their properties by means of molecular design and other physical properties. The main disadvantage of these materials is the fact that the high value of hyperpolarizability β often occurs with high dipole moment which leads to a tendency of the molecules to form a centrosymmetric assembly. To this group belong compounds containing one aromatic ring with substituents of electron donor/acceptor nature such as nitroanilines,[6] for instance 2-methyl-4-nitroaniline (MNA) or *N*,*N*'-dimethyl-4-nitroaniline. Further, the compounds with two aromatic rings connected through a system of conjugated double bonds also belong here. An example of such assembly is 4'-dimethylamino-N-methyl-4-stilbazoliumtosylate (DAST).[7] Next representatives are the "pull-push" ethylenes[8] or the simple molecules as urea.[9]

The third group includes materials which combine the advantages of previously mentioned groups. Holders of the NLO properties are the organic molecules, nevertheless, the non-symmetric assembly is obtained thanks to the formation of their salts and co-crystals. So this concept of functional salts consists of anions that are important resources of the structure assembly (forming chains or networks *via* hydrogen bonds or even in case of chiral organic anions directing the non-centrosymmetric assembly) and cations responsible for NLO properties.[1, 5] To this group belong salts of argininium(1+)[10, 11] – *e.g.* argininium(1+) dihydrogen phosphate monohydrate (LAP).[5] Other examples are the salts and co-crystals of guanazole,[12] triphenylamine,[13]2-aminopyrimidine, substituted pyridines[14] as 4-aminopyridine, 2-(N-prolinol)-5-nitropyridine (PNP)[14] and 2-hydroxypyridine.

3.4 2,4-diamino-1,3,5-triazine

The 2,4-diamino-1,3,5-triazine (**DAMT**), also called guanamine, is another heteroaromatic compound studied in our research group for its potential to form salts or adducts with expected NLO properties. The utilization of this molecule as NLO material has not been studied yet. Nevertheless, the derivate of guanamine – 2,4-diamino-6-phenyl-1,3,5-triazine – was used as a starting material for three novel triazine based organic "push-pull" chromophores in the field of NLO.[15, 16]

The first published study regarding to 2,4-diamino-1,3,5-triazine was the investigation of its structure and the properties along with ammeline and melamine by *ab initio* methods. Resulting molecular structure of 2,4-diamino-1,3,5-triazine have been determined at the SCF-level using three different basis sets.[17]

Nowadays also the X-ray crystal structure of 2,4-diamino-1,3,5-triazine is available.[18] Based on single crystal X-ray analysis it was found that chemical formula for this compound is $C_3H_5N_5$ and relative molecular mass is 111.12. The product crystallizes in monoclinic system with space group $P2_1/c$ (a = 9.8631(9) Å, b = 3.7180(3) Å, c = 12.9609(9) Å, β = 99.643(9)°, V = 468.57(7) Å^3). This structural analysis was performed within the study of 2,4-diamino-1,3,5-triazine as a prospective candidate to mimic base-pairing of nucleic acids.[18]

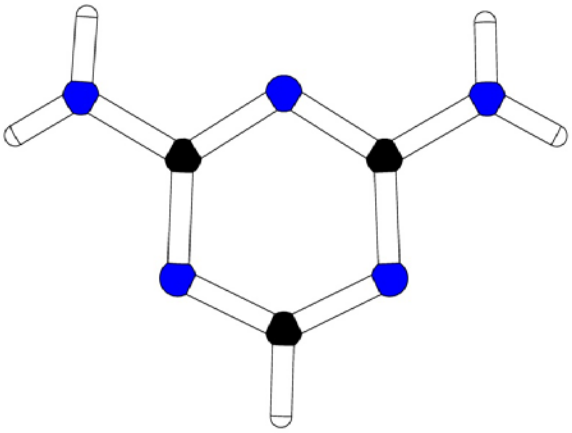

Figure 1: Asymmetric unit of **DAMT**.

The asymmetric unit of 2,4-diamino-1,3,5-triazine contains a planar molecule which is shown in Figure 1. Moreover, molecules of 2,4-diamino-1,3,5-triazine are associated in the crystal structure *via* N–H…N hydrogen bonds to form 3D framework as seen in Figure 2. The molecular geometry of the aromatic ring conforms to C_{2v} symmetry within experimental error.[18]

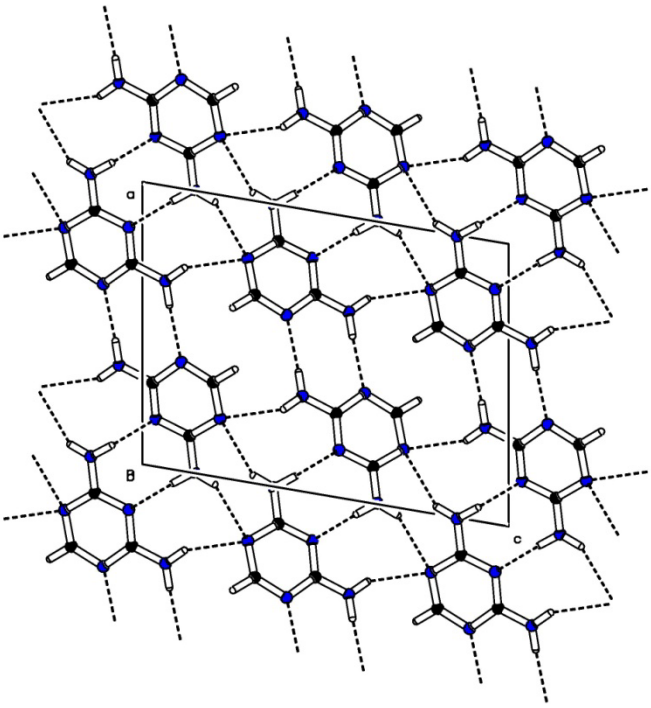

Figure 2: Crystal packing of **DAMT**, view along the crystallographic axis *b*. The dashed lines indicate the hydrogen bonds.

The infrared and Raman spectra have not been studied till now and that is why they are also included in this thesis. Similarly, no literature source mentions any salt or adduct of 2,4-diamino-1,3,5-triazine yet.

4 Aim of thesis

The aim of this thesis is to study and explore the systems of 2,4-diamino-1,3,5-triazine with selected inorganic and organic acids in search of novel compounds with expected NLO properties and, subsequently, characterization of obtained materials using methods of vibrational spectroscopy, powder X-ray diffraction and single crystal X-ray analysis.

Moreover, the compounds fulfilling symmetry conditions will be selected for investigating of their second harmonic generation efficiency.

5 Experimental part

5.1 Preparation of compounds of 2,4-diamino-1,3,5-triazine with inorganic acids

For the preparations of salts of 2,4-diamino-1,3,5-triazine following acids were used: nitric acid (65%, p. a., Lach-Ner), sulfuric acid (96%, p. a., Lach-Ner), phosphoric acid (85%, Lachema), phosphorous acid (Merck), perchloric acid (70%, Merck) and hydrochloric acid (35%, p. a., Lach-Ner). The products were obtained by crystallization of solutions prepared by dissolving of 0.1 g of 2,4-diamino-1,3,5-triazine (98%, Aldrich) in the amount of acid (1mol/l) corresponding to stoichiometry described in Table 3 (chapter 6.2, page 17) and distilled water needed for dissolving of organic base (approximately 10 ml). The molar ratio of base/acid was chosen with respect to expected stoichiometry of the product.

5.2 Preparation of compounds of 2,4-diamino-1,3,5-triazine with organic acids

The process of salts preparation was the same as described in part 5.1. Following acids were used: 2 mol/l formic acid (85–87%, Lachema), 0.5 mol/l malonic acid (pure, Reachim), 0.5 mol/l succinic acid (p. a., Lachema), 0.5 mol/l glutaric acid (96%, Fluka), 0.15 mol/l adipic acid, 2 mol/l L–malic acid (97%, Aldrich) and 2 mol/l L–tartaric acid (99.5%, Aldrich). The products are listed in Table 16 (chapter 6.3, page 34).

5.3 Methods of characterization

5.3.1 FTIR spectroscopy

The infrared spectra were recorded at the room temperature using nujol and flourolube mulls (KBr windows) technique on a Nicolet 6700 FTIR spectrometer with 2 cm^{-1} resolution and Happ–Genzel apodization in the 400–4000 cm^{-1} region.

5.3.2 FT Raman spectroscopy

The Raman spectra of polycrystalline samples were recorded at the room temperature on a Nicolet 6700 FTIR spectrometer equipped with a Nexus FT Raman module (2 cm^{-1} resolution, Happ–Genzel apodization, 1064 nm Nd:YVO_4 laser excitation, 500 mW power at the sample) in the 150–3700 cm^{-1} region. All presented spectra were processed in OMNIC software.[19]

5.3.3 Single crystal X-ray analysis

The single crystal X-ray diffraction data were performed on a Nonius Kappa diffractometer (Mo Kα radiation, λ = 0.71073 Å, graphite monochromator) equipped with Bruker Apex-II CCD array detector. The basic crystallographic data, information about measurement refinement parameters are included in CIF files. The CIF files of presented crystal structures are available on the appended CD – ROM. For further processing and figures generation programme Platon[20] was used.

5.3.4 Powder X-ray diffraction

The powder diffraction data were collected on X'Pert PRO (PANalytical) diffractometer with CuK_α lamp (λ = 1.54278 Å). The 2θ range was set from 5° to 60° with the step 0.013°. The data were processed by using X'Pert HighScore software.[21]

5.3.5 SHG measurements

The measurements of SHG at 800 nm were carried out with 100 fs laser pulses generated at an 82 MHz repetition rate by an Ti:sapphire laser (MaiTai, Spectra Physics). For quantitative determination of the SGH efficiency the intensity of the back-scattered laser light at 400 nm generated in the sample was measured by a grating spectrograph with diode array (InstaSpec II, Oriel) and the signal was compared with that one generated in KDP (KH_2PO_4). The experiment was performed using powdered samples (100 – 150 μm particle size) loaded into 5mm glass cells with the aid of a vibrator and the measurements were repeated on different areas of the sample. Each of the samples was measured seven times on different areas of the same sample to minimize the signal fluctuation induced by sample packing and the results were averaged while the outlying values were excluded.

5.3.6 Quantum – chemical calculations

Quantum – chemical calculations (GAUSSIAN09W[22]) of **DAMT** and **DAMT(1+)** cation were performed employing the closed-shell restricted density functional method (B3LYP) with the 6-311+G (d, p) basis set. The visualization of the results was carried out with the GaussView[23] program package. The geometry optimizations, also yielding the molecular energies, were followed by frequency calculation together with IR intensities and Raman activities using the same method and the basis set.

6 Results

6.1 Characterization of 2,4-diamino-1,3,5-triazine

Before the beginning of our work with this base the basic characterization measurements were performed. The IR and Raman spectra are depicted in Figure 3. The values of vibrational frequencies were read from the spectra and they are listed in Table 1. The base was also characterized by powder X-ray diffraction and selected diffraction maxima are listed in Table 2.

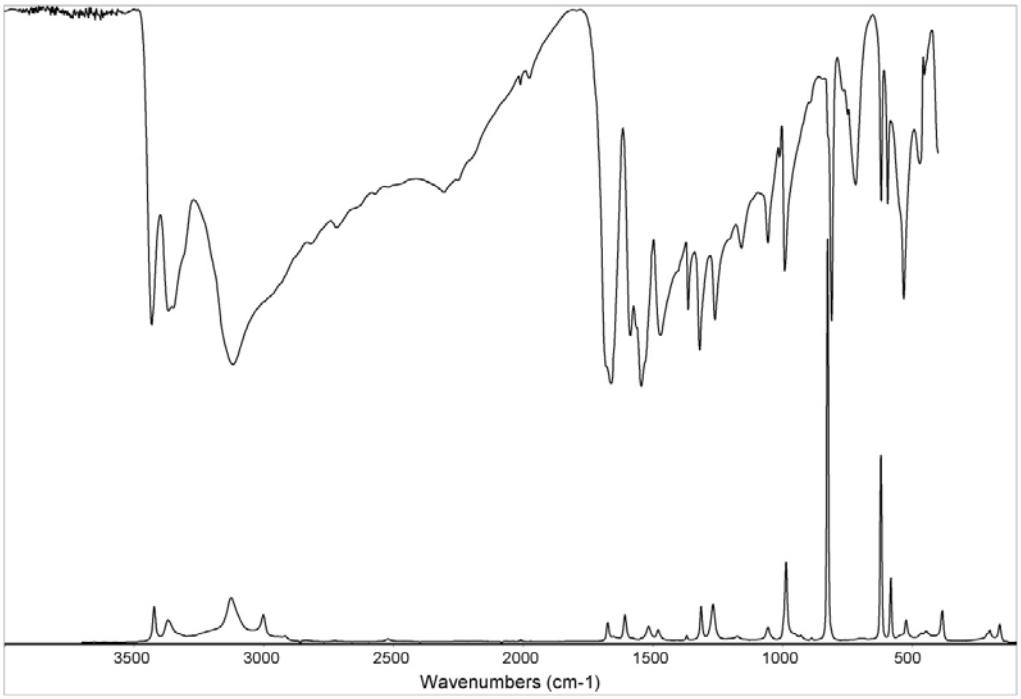

Figure 3: IR (compiled from nujol and fluorolube mulls) and Raman spectra of **DAMT.**

Table 1: Recorded vibrational frequencies of **DAMT**.

IR (cm^{-1})			Raman (cm^{-1})		
3433 m	1587 m	992 m	3423 w	1372 w	524 w
3368 m	1545 s	811 m	3371 w	1314 w	386 w
3349 m	1472 m	719 w	3126 w	1268 w	203 w
3120 s	1364 m	620 w	3002 w	1057 w	165 w
2720 w	1320 m	594 w	1674 w	986 w	
2300 w	1261 m	532 m	1608 w	826 s	
1970 w	1159 w	471 w	1516 w	620 m	
1661 s	1057 w	453 w	1481 w	582 w	

Table 2: Selected diffraction maxima and d-spacing for **DAMT.**

Position (°2θ)	d-spacing (Å)	Rel. Int. (%)	Position (°2θ)	d-spacing (Å)	Rel. Int. (%)
9.128	9.689	6.04	29.960	2.980	33.91
13.903	6.370	28.87	30.047	2.979	21.20
15.301	5.791	100.00	36.244	2.483	4.15
17.874	4.963	70.12	41.869	2.156	6.95
18.264	4.858	20.15	41.987	2.155	3.67
24.890	3.577	11.98	46.947	1.934	3.89
25.591	3.481	48.34	47.075	1.934	2.06
26.947	3.309	37.32	49.712	1.833	1.21
27.707	3.220	9.78	55.484	1.655	1.48
27.915	3.196	16.65	57.631	1.589	1.13

6.2 Systems containing DAMT and inorganic acids

This part contains the results of crystallization of 2,4-diamino-1,3,5-triazine with inorganic acids. The studied systems are presented in Table 3. The chapter describes the structures of the salts and also data from all measurements (vibrational spectroscopy and powder X-ray diffraction) are included.

Table 3: Systems of 2,4-diamino-1,3,5-triazine with inorganic acids.

Acid	Ratio	Product	Acid	Ratio	Product
HNO_3	1:1	**DAMT NO_3**	H_3PO_4	1:1	**DAMT H_2PO_4**
	1:2	**DAMT NO_3**		1:2	**DAMT H_2PO_4**
	2:1	**DAMT**		1:3	**DAMT H_2PO_4**
H_2SO_4	1:1	**$(DAMT)_2$ $SO_4 \cdot H_2O$**	$HClO_4$	1:1	**$(DAMT)_2$ $ClO_4 \cdot 2H_2O$**
	2:1	**$(DAMT)_2$ $SO_4 \cdot H_2O$**		1:2	**$(DAMT)_2$ $ClO_4 \cdot 2H_2O$**
	3:1	**$(DAMT)_2$ $SO_4 \cdot H_2O$**		1:3	**$(DAMT)_2$ $ClO_4 \cdot 2H_2O$**
	1:2	**$(DAMT)_2$ $SO_4 \cdot H_2O$**		2:1	**DAMT**
	1:3	**$(DAMT)_2$ $SO_4 \cdot H_2O$**		2:3	**$(DAMT)_2$ $ClO_4 \cdot 2H_2O$**
H_3PO_3	1:1	**DAMT H_2PO_3**		3:2	**DAMT**
	1:2	**DAMT H_2PO_3**	HCl	1:1	**DAMT Cl**

2,4-diamino-1,3,5-triazinium(1+) nitrate – product **DAMT NO_3**

This product was obtained from the solutions containing 2,4-diamino-1,3,5-triazine and nitric acid in molar ratios 1:1 and 1:2 (see Table 3). Based on single crystal X-ray analysis it was found that chemical formula for this compound is $C_3H_6N_6O_3$ and relative molecular mass is 174.14. The product crystallizes in monoclinic system with space group $P2_1/n$ (a = 6.8407(4) Å, b = 9.6507(5) Å, c = 10.3787(6) Å, β = 98.013(2)°, V = 678.49(7) Å^3).

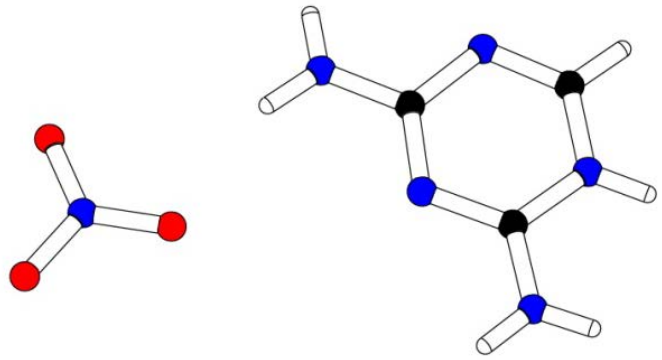

Figure 4: Asymmetric unit of **DAMT NO_3** (C – black, N – blue, O – red).

The crystal structure of **DAMT NO_3** consists of the 2,4-diamino-1,3,5-triazinium(1+) cations formed to the chains which are connected *via* N–H…N hydrogen bonds. These bonds are formed between NH_2 group and the nitrogen atom from the aromatic ring. These chains of cations are interconnected by nitrate anions *via* N–H…O hydrogen bonds and it forms a layered structure as seen in Figure 5.

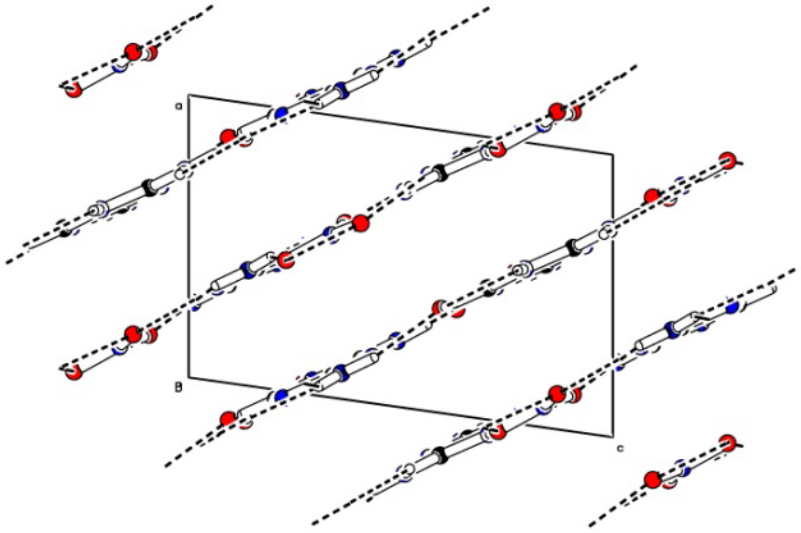

Figure 5: Crystal packing of **DAMT NO_3**, view along the crystallographic axis *b*. The dashed lines indicate the hydrogen bonds.

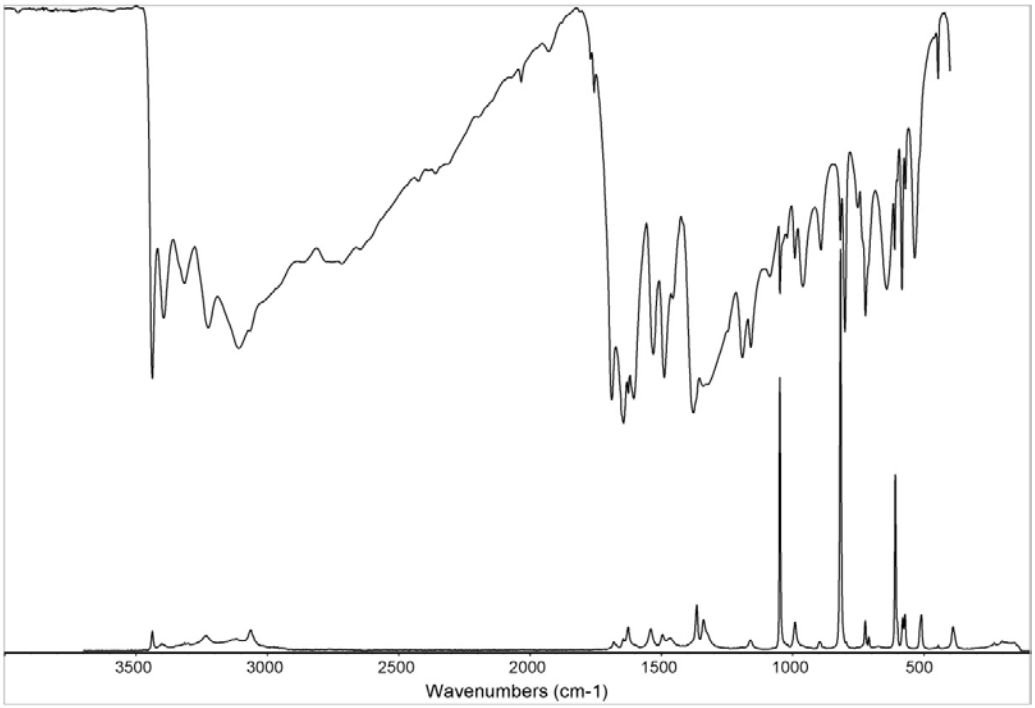

Figure 6: IR (compiled from nujol and fluorolube mulls) and Raman spectra of **DAMT NO_3**.

The sample was also characterized by vibrational spectroscopy. The IR and Raman spectra are depicted in Figure 6. The values of vibrational frequencies were read from the spectra and they are listed in Table 4. Bolded values are vibrational frequencies of nitrate anion. Some of them are also overlapped by vibrational manifestations of **DAMT(1+)** cation. This basic assignment is based on available literature.[24]

Table 4: Recorded vibrational frequencies of **DAMT NO_3**.

IR (cm^{-1})			Raman (cm^{-1})	
3438 m	1531 m	893 w	3438 w	991 w
3395 m	1489 m	**819 w**	3063 w	895 w
3316 w	1454 w	801 m	1681 w	**818 s**
3225 m	**1378 s**	756 w	1627 w	**724 w**
3110 m	1341 w	**723 m**	1541 w	709 w
2034 w	1192 m	643 m	1495 w	609 m
1760 w	1086 w	612 w	1463 w	586 w
1689 m	1160 m	584 m	**1365 w**	573 w
1644 s	**1048 w**	571 w	1339 w	510 w
1626 m	992 w	536 m	1163 w	388 w
1605 m	962 w	446 w	**1048 s**	

The product was also characterized by powder X-ray diffraction. Selected diffraction maxima were read from the pattern and they are listed in Table 5.

Table 5: Selected diffraction maxima and d-spacing for **DAMT NO_3**.

Position (°2θ)	d-spacing (Å)	Rel. Int. (%)	Position (°2θ)	d-spacing (Å)	Rel. Int. (%)
14.424	6.141	0.18	27.974	3.190	0.49
17.098	5.186	0.94	28.978	3.079	100.00
17.300	5.126	1.67	29.064	3.077	47.09
19.589	4.532	1.84	30.148	2.962	0.20
24.885	3.578	0.11	33.054	2.708	0.12
25.328	3.516	0.16	34.512	2.597	0.19
25.973	3.431	0.70	41.541	2.172	0.55
26.177	3.404	0.33	45.064	2.010	0.17
27.583	3.234	1.20	53.547	1.710	0.12
27.770	3.213	1.80	54.451	1.684	0.13

bis(2,4-diamino-1,3,5-triazinium(1+)) sulfate monohydrate – product **$(DAMT)_2\ SO_4 \cdot H_2O$**

As listed in Table 3, the product **$(DAMT)_2\ SO_4 \cdot H_2O$** yields in all prepared molar ratios of base and acid. Chemical formula of this product is $C_3H_8N_5O_{2,5}S$ and relative molecular mass is 186.20. The salt belongs to orthorhombic system with space group *Pbcn* (*a* = 17.4155(4) Å, *b* = 11.4943(3) Å, *c* = 6.7785(2) Å, *V* = 1356.91(6) $Å^3$).

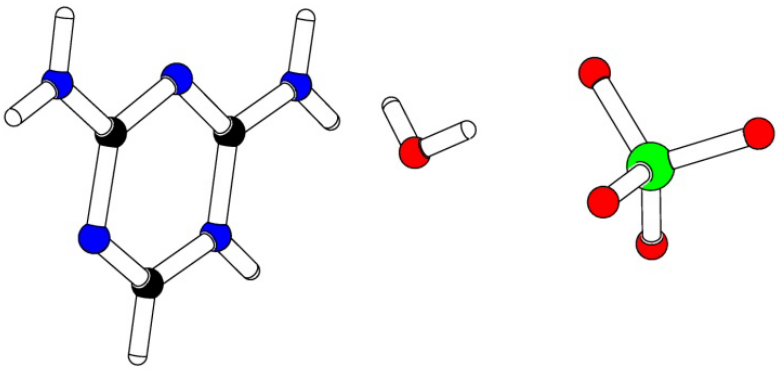

Figure 7: Asymmetric unit of **$(DAMT)_2\ SO_4 \cdot H_2O$** (C – black, N – blue, O – red, S – green).

The structure consists of the cationic chains where the cations of **DAMT(1+)** are connected *via* N–H…N hydrogen bonds. NH_2 group is connected *via* this type of hydrogen

bond with the nitrogen atom from the aromatic ring. These chains are located in the plane *ab*. In the plane *bc* there are located the chains formed by alternating molecules of sulfate anions and molecules of water connected *via* O–H…O hydrogen bonds. These cationic and anionic chains are interconnected together *via* N–H…O hydrogen bonds to form a 3D network. The molar ratio of **DAMT(1+)** to sulfate anion is 2:1.

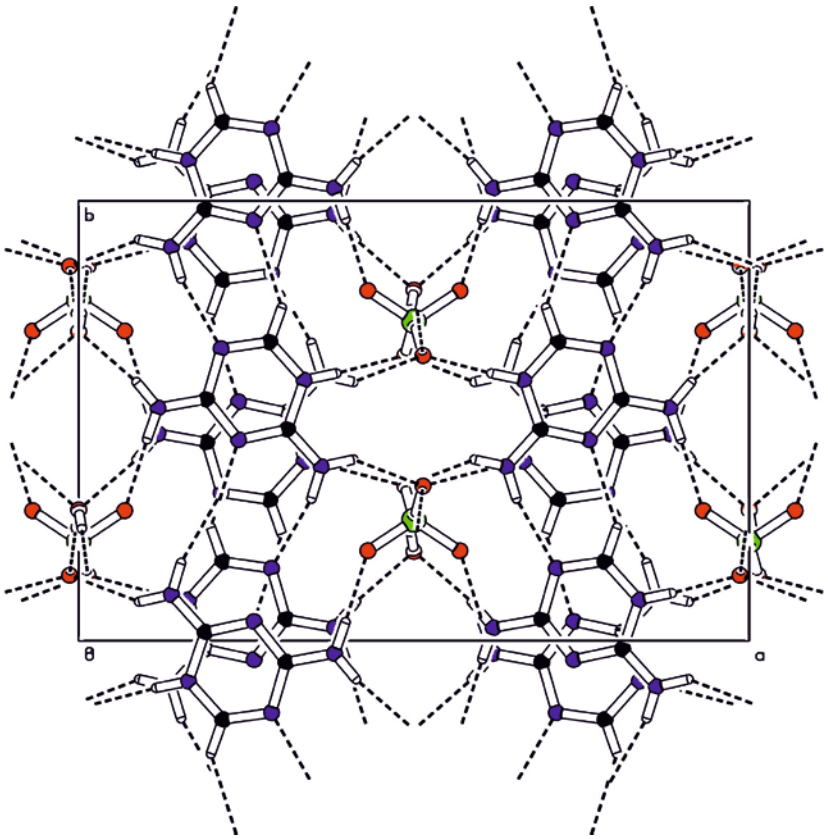

Figure 8: Crystal packing of **$(DAMT)_2\ SO_4 \cdot H_2O$**, view along the crystallographic axis *c*. The dashed lines indicate the hydrogen bonds.

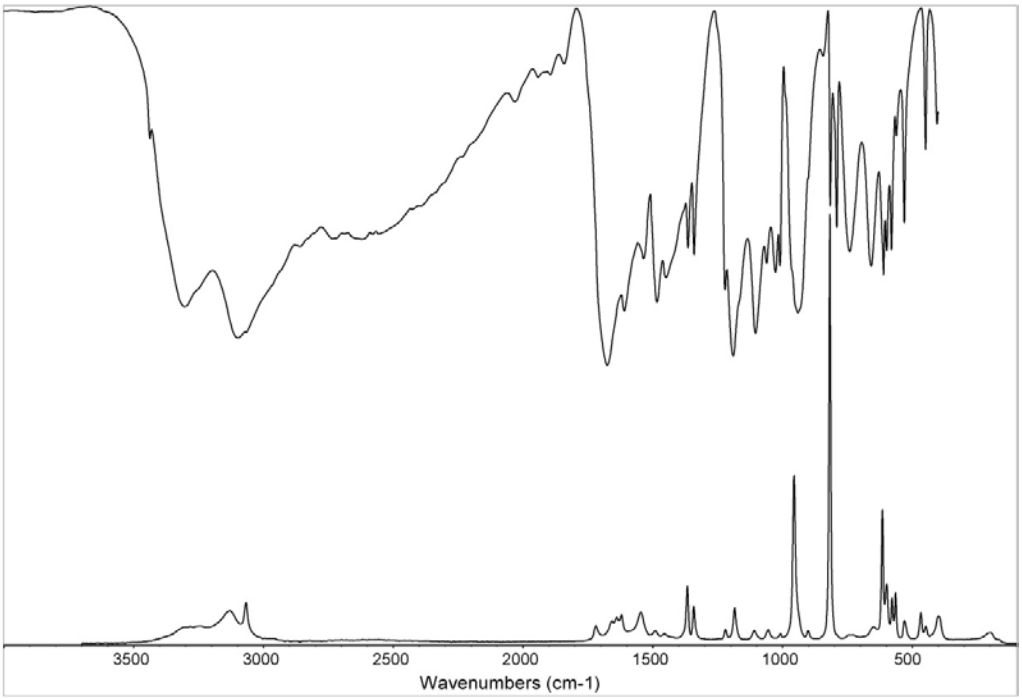

Figure 9: IR (compiled from nujol and fluorolube mulls) and Raman spectra of **$(DAMT)_2\ SO_4 \cdot H_2O$**.

The IR and Raman spectra are depicted in Figure 9. The values of vibrational frequencies were read from the spectra and they are listed in Table 6. Bolded values are vibrational frequencies of sulfate anion. Some of them are also assigned to the vibrational modes of **DAMT(1+)** cation. This basic assignment is based on available literature.[24]

Table 6: Recorded vibrational frequencies of **$(DAMT)_2\ SO_4 \cdot H_2O$**.

IR (cm^{-1})			Raman (cm^{-1})		
3438 w	1341 w	791 w	3068 w	1183 w	564 w
3304 w	1222 w	**740 m**	1722 w	**1110 w**	531 w
3110 s	**1190 s**	660 m	1660 w	1054 w	**467 w**
1845 w	**1104 s**	**611 m**	1643 w	**956 m**	450 w
1676 s	1061 w	599 w	1621 w	904 w	394 w
1610 m	1028 w	559 w	1546 w	818 s	200 w
1537 w	1010 w	531 w	1489 w	653 w	
1485 m	**942 m**	448 w	1367 w	**615 m**	
1450 w	847 w		1342 w	599 w	
1365 w	816 w		1219 w	578 w	

The product was also characterized by powder X-ray diffraction. Selected diffraction maxima were read from the pattern and they are listed in Table 7.

Table 7: Selected diffraction maxima and d-spacing for **$(DAMT)_2\ SO_4 \cdot H_2O$**.

Position (°2θ)	d-spacing (Å)	Rel. Int. (%)	Position (°2θ)	d-spacing (Å)	Rel. Int. (%)
9.290	9.520	5.32	27.780	3.209	22.91
15.998	5.540	44.28	28.123	3.170	7.10
18.536	4.787	63.20	30.922	2.890	8.78
20.234	4.389	14.26	32.217	2.777	8.08
20.878	4.255	6.65	39.808	2.263	6.56
21.571	4.120	12.62	43.335	2.086	1.05
25.693	3.467	13.84	50.318	1.812	0.69
26.144	3.409	16.84	54.820	1.673	2.75
26.661	3.341	100.00	54.949	1.674	1.57
26.746	3.339	41.34	55.438	1.656	1.93
27.185	3.278	9.01	59.268	1.558	0.94

2,4-diamino-1,3,5-triazinium(1+) hydrogen phosphite – product **(DAMT H_2PO_3)**

The product **DAMT H_2PO_3** crystallizes from the base/acid molar ratio 1:1 as well as 1:2. Chemical formula is $C_4H_7N_3O_4P$, relative molecular mass is 192.10. The compound crystallizes in monoclinic system with space group $P2_1/n$ (a = 13.0250(3) Å, b = 4.4966(2) Å, c = 13.3799(4) Å, β = 101.748(1)°, V = 784.28(5) Å).

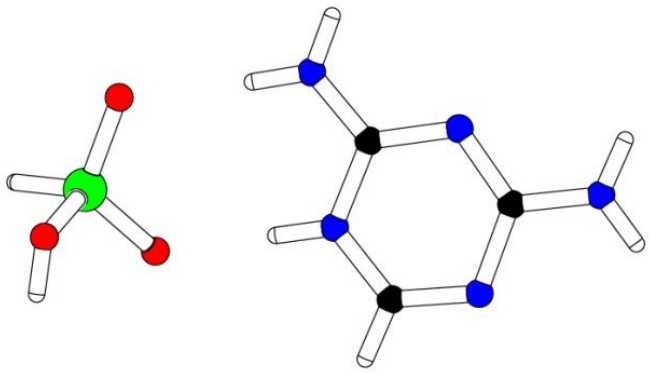

Figure 10: Asymmetric unit of **DAMT H_2PO_3** (C – black, N – blue, O – red, P – green).

The crystal structure consists of the centrosymmetric pairs of **DAMT(1+)** cations connected *via* two N–H…N hydrogen bonds where NH_2 group is connected with nitrogen

atom from the ring which is placed between the two substituted carbon atoms (see Figure 11) and pairs of phosphite anions connected *via* O–H…O hydrogen bonds. These fragments are interconnected to 3D network *via* N–H…O hydrogen bonds.

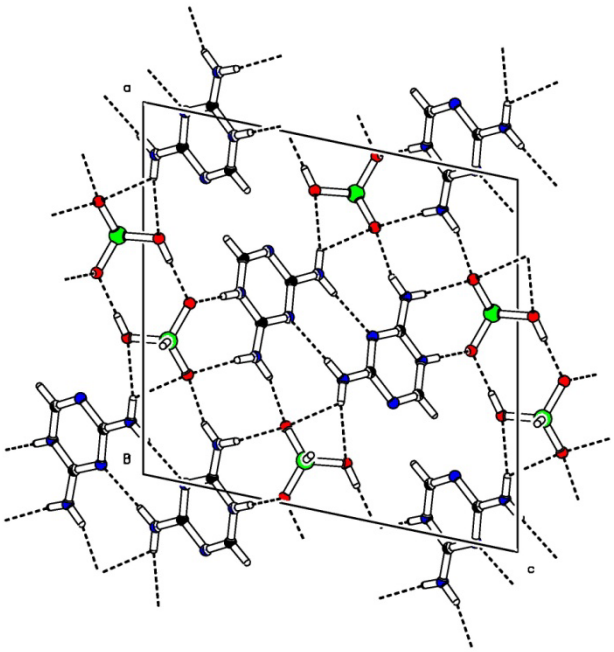

Figure 11: Crystal packing of **DAMT H_2PO_3**, view along the crystallographic axis *b*. The dashed lines indicate the hydrogen bonds.

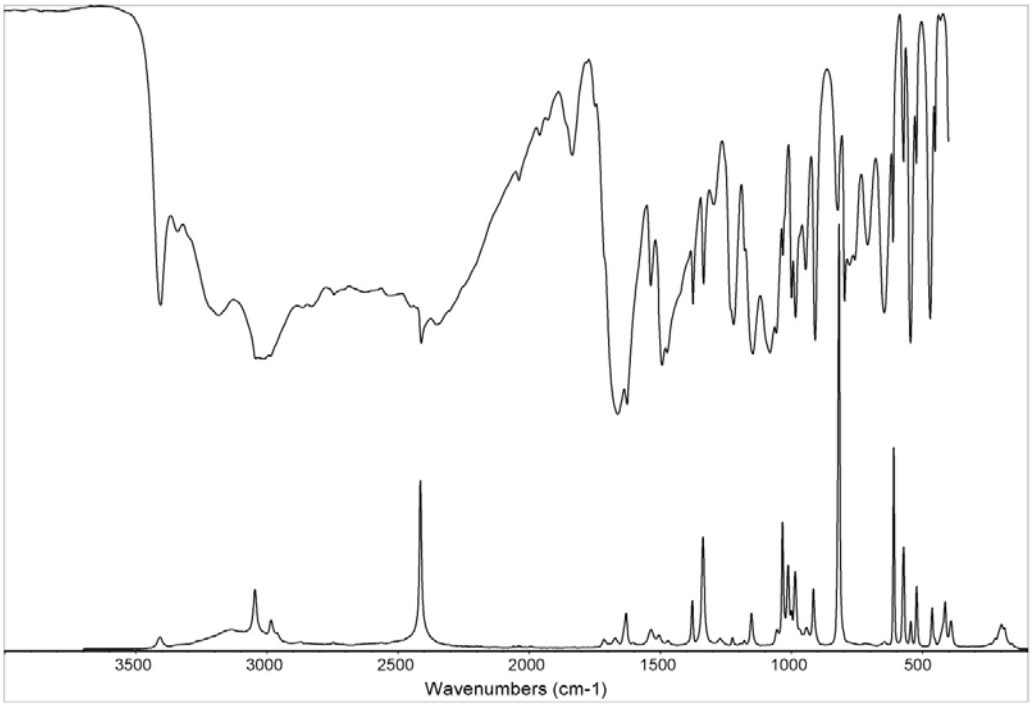

Figure 12: IR (compiled from nujol and fluorolube mulls) and Raman spectra of **DAMT H_2PO_3**.

The IR and Raman spectra are depicted in Figure 12. The values of vibrational frequencies were read from the spectra and they are listed in Table 8. Bolded values are vibrational frequencies of phosphite anion. Most of them are also peaks belonged to vibrational modes of **DAMT(1+)** cation because of their overlapping. This assignment is based on available literature.[24, 25, 26]

Table 8: Recorded vibrational frequencies of **DAMT H_2PO_3**.

IR (cm^{-1})			Raman (cm^{-1})		
3406 m	1335 w	797 m	3409 w	**1152 w**	**414 w**
3341 w	1298 w	777 w	3046 w	**1034 m**	394 w
3185 m	**1221 m**	710 w	2985 w	**1012 w**	200 w
3010 m	**1148 m**	647 m	**2415 m**	986 w	
2412 m	1082 m	613 w	1716 w	942 w	
2045 w	**1056 w**	**573 w**	1675 w	**916 w**	
1836 w	**1033 w**	**546 m**	1630 w	818 s	
1663 s	1000 m	**524 w**	1536 w	609 m	
1627 s	985 m	471 m	1378 w	**572 w**	
1537 w	946 w	452 w	1337 m	**545 w**	
1494 m	**910 m**		1272 w	**522 w**	
1375 w	823 w		**1224 w**	463 w	

The product was also characterized by powder X-ray diffraction. Selected diffraction maxima were read from the pattern and they are listed in Table 9.

Table 9: Recorded diffraction maxima and d-spacing for **DAMT H_2PO_3**.

Position (°2θ)	d-spacing (Å)	Rel. Int. (%)	Position (°2θ)	d-spacing (Å)	Rel. Int. (%)
13.933	6.356	27.58	28.581	3.123	12.09
17.411	5.094	94.85	29.861	2.990	24.07
20.505	4.331	32.83	29.937	2.990	20.97
21.201	4.191	6.72	33.052	2.708	12.84
22.081	4.026	7.76	33.445	2.677	6.56
22.678	3.921	14.41	35.122	2.553	11.15
23.192	3.853	7.01	39.173	2.298	3.15
23.624	3.766	20.97	40.687	2.216	3.68
23.878	3.727	22.92	42.399	2.130	2.88
25.389	3.508	100.00	48.762	1.866	3.57
27.948	3.193	17.72	53.214	1.720	3.40
28.138	3.171	6.97	57.631	1.598	1.61

2,4-diamino-1,3,5-triazonium(1+) dihydrogen phosphate – product **(DAMT H_2PO_4)**

The product crystallizes in all ratios (see Table 3) as dihydrogen phosphate. Chemical formula of **DAMT H_2PO_4** is $C_6H_{15}N_{10}O_8P_2$, relative molecular mass is 417.22. This salt crystallizes in triclinic system with space group *P*–1 (a = 9.0214(2) Å, b = 9.2861(2) Å, c = 10.2988(3) Å, α = 84.819(1)°, β = 67.732(1)°, γ = 83.694(1) Å, V = 792.48(3) Å^3).

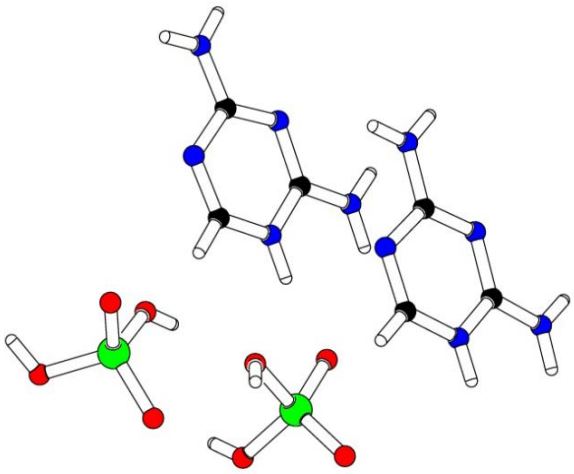

Figure 13: Asymmetric unit of **DAMT H_2PO_4** (C – black, N – blue, O – red, P – green).

The structure consists of **DAMT(1+)** cations connected *via* two N–H…N hydrogen bonds where NH_2 group is connected with a nitrogen atom from the ring to the chains.

Anions form the layers which are interconnected together by cationic chains *via* N–H…O hydrogen bonds to form 3D network. Additionally, anions themselves are connected *via* O–H…O hydrogen bonds.

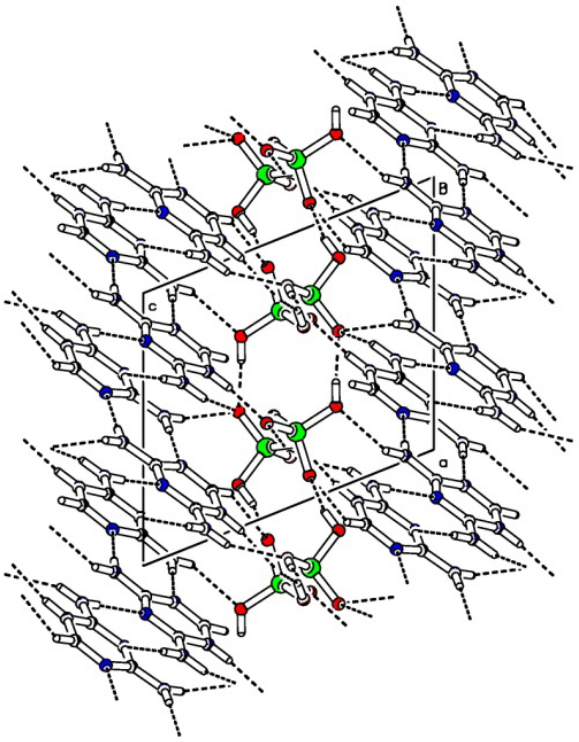

Figure 14: Crystal packing of **DAMT H_2PO_4,** view along the crystallographic axis *b*. The dashed lines indicate the hydrogen bonds.

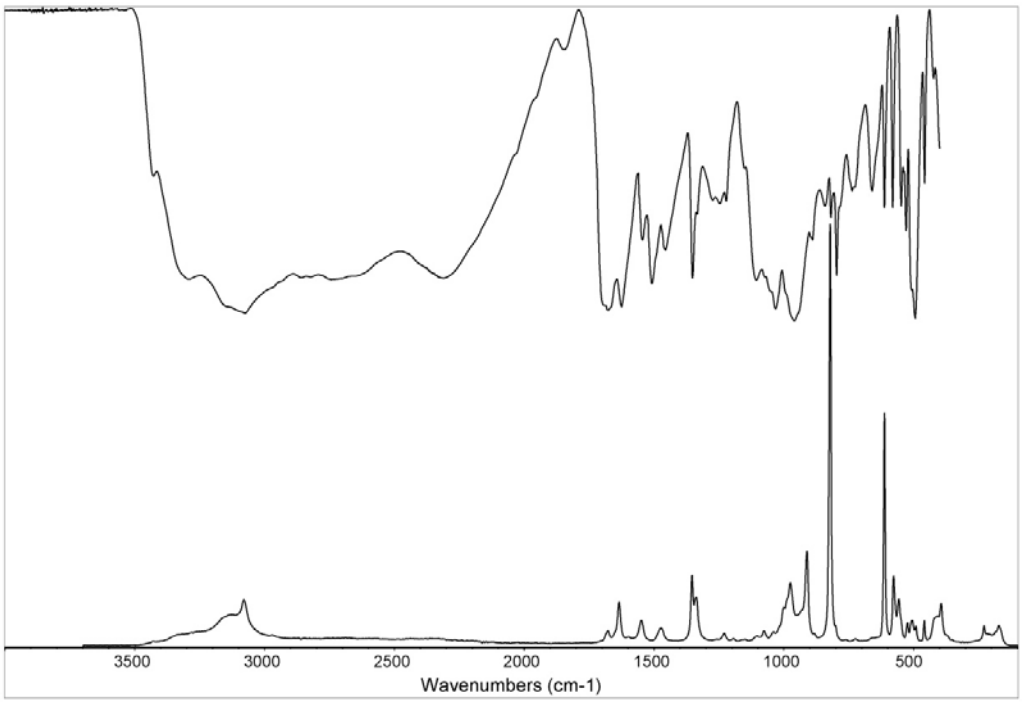

Figure 15: IR (compiled from nujol and fluorolube mulls) and Raman spectra of **DAMT H_2PO_4**.

The IR and Raman spectra are depicted in Figure 15. The values of vibrational frequencies were read from the spectra and they are listed in Table 10. Bolded values are vibrational frequencies of phosphate anion which could be overlapped by the vibrational frequencies of **DAMT(1+)** cation. This assignment is based on available literature.[24, 25]

Table 10: Recorded vibrational frequencies of **DAMT H_2PO_4**.

IR (cm^{-1})			Raman (cm^{-1})		
3429 w	1456 w	796 m	3081 w	**975 w**	397 w
3290 m	**1352 m**	737 w	1678 w	**911 w**	232 w
3070 s	1247 w	660 w	1635 w	822 s	173 w
2310 m	**1107 m**	613 w	1549 w	612 m	
1845 w	1032 s	581 w	1472 w	577 w	
1675 s	**961 s**	**548 w**	**1353 w**	**557 w**	
1625 s	**892 w**	**529 w**	**1339 w**	**524 w**	
1544 w	842 w	**494 s**	1230 w	509 w	
1509 m	819 w	458 w	1077 w	459 w	

The product was also characterized by powder X-ray diffraction. Selected diffraction maxima were read from the pattern and they are listed in Table 11.

Table 11: Selected diffraction maxima and d-spacing for **DAMT H_2PO_4**.

Position (°2θ)	d-spacing (Å)	Rel. Int. (%)	Position (°2θ)	d-spacing (Å)	Rel. Int. (%)
9.357	9.452	35.01	26.505	3.363	14.78
13.127	6.745	4.48	27.924	3.193	23.57
18.636	4.761	51.80	28.023	3.184	36.41
19.251	4.611	41.97	28.331	3.150	7.28
20.495	4.334	31.97	30.570	2.922	17.09
21.127	4.205	9.60	30.649	2.917	19.25
21.404	4.151	36.63	33.319	2.689	7.62
22.367	3.975	32.52	33.912	2.643	7.31
22.732	3.912	10.53	38.696	2.327	6.73
23.329	3.813	14.65	45.454	1.995	4.47
25.334	3.516	100.00	51.935	1.759	2.41
26.170	3.405	14.12	52.147	1.754	2.36

2,4-diamino-1,3,5-triazine 2,4-diamino-1,3,5-triazinium(1+) perchlorate dihydrate – product **($(DAMT)_2\ ClO_4 \cdot 2H_2O$)**

The product **$(DAMT)_2\ ClO_4 \cdot 2H_2O$** crystallizes in all ratios listed in Table 3. The ratio of 2,4-diamino-1,3,5-triazine and perchloric acid in the product is 2:1 as seen in Figure 16. Chemical formula of this compound is $C_{18}HCl_5N_{11}O_6$, relative molecular mass is 644.55. The salt crystallizes in triclinic system with space group *P*–1 (a = 7.5629(2) Å, b = 9.2967(2) Å, c = 10.9263(3) Å, α = 94.147(1)°, β = 107.712(1)°, γ = 100.516(1)°, V = 712.79(3) Å^3).

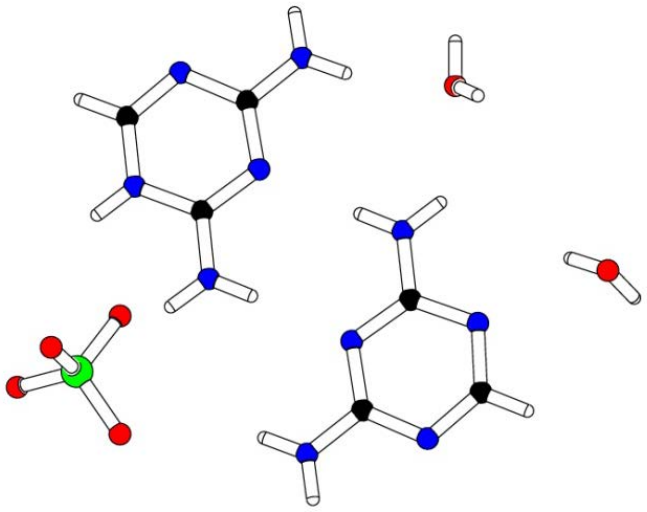

Figure 16: Asymmetric unit of **$(DAMT)_2\ ClO_4 \cdot 2H_2O$**
(C – black, N – blue, O – red, Cl – green).

The structure contains **DAMT(1+)** cations as well as uncharged molecules of **DAMT**. They are connected together *via* N–H…N hydrogen bonds and form chains interconnected with anions and molecules of water *via* N–H…O and O–H…N hydrogen bonds to 3D network. Perchlorate anions and molecules of water are connected *via* O–H…O hydrogen bonds to form chains where they alternate.

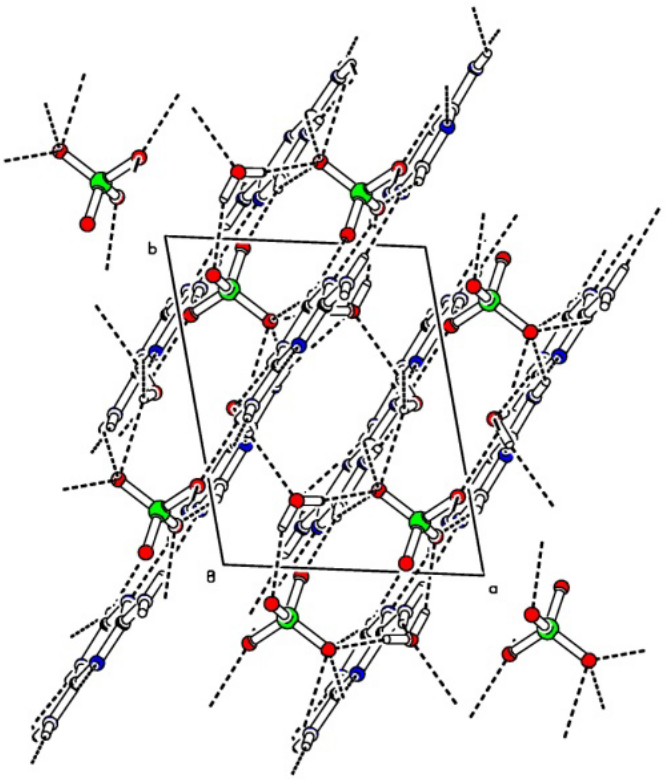

Figure 17: Crystal packing of **$(DAMT)_2\ ClO_4 \cdot 2H_2O$**, view along the crystallographic axis *c*. The dashed lines indicate the hydrogen bonds.

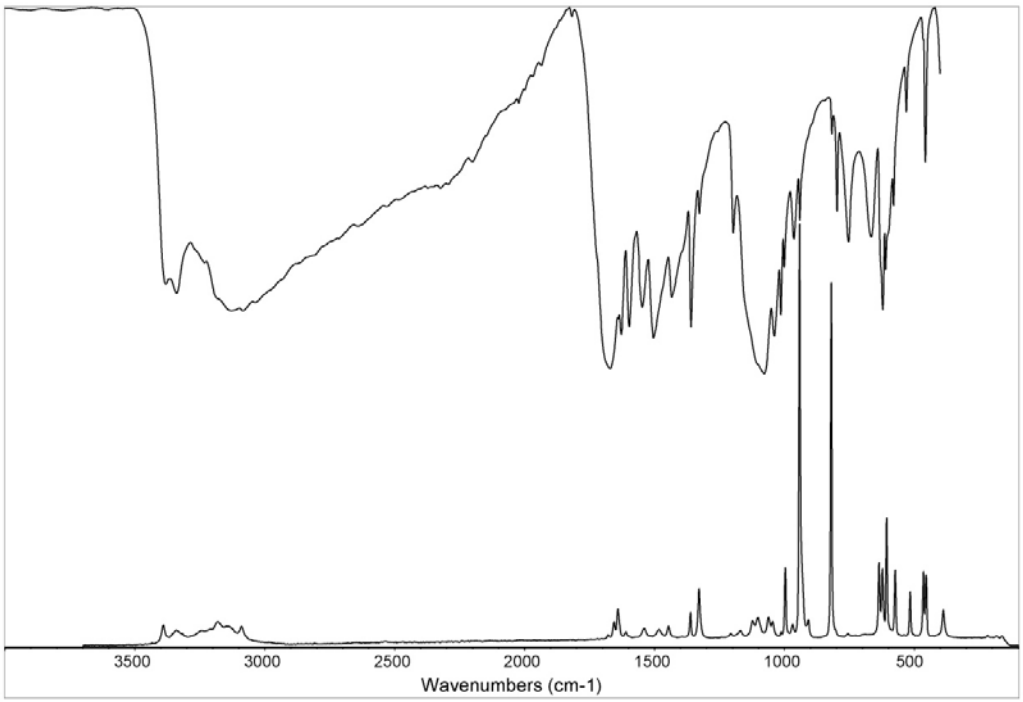

Figure 18: IR (compiled from nujol and fluorolube mulls) and Raman spectra of **$(DAMT)_2\ ClO_4 \cdot 2H_2O$**.

The IR and Raman spectra are depicted in Figure 18. The values of vibrational frequencies were read from the spectra and they are listed in Table 12. Bolded values are vibrational frequencies of perchlorate anion. Some of them are overlapped by the vibrational modes of **DAMT** and/or its cation. This assignment is based on available literature.[24, 25]

Table 12: Recorded vibrational frequencies of **$(DAMT)_2\ ClO_4 \cdot 2H_2O$**.

IR (cm^{-1})			Raman (cm^{-1})		
3382 m	1359 m	797 w	3391 w	1328 w	**623 w**
3340 m	1327 w	753 w	3340 w	1170 w	606 m
3130 m	1197 w	666 w	3185 w	**1125 w**	573 w
3080 m	**1078 s**	**621 m**	3091 w	**1102 w**	516 w
1671 s	1040 m	610 w	1657 w	1062 w	**465 w**
1628 m	1014 m	580 w	1641 w	1045 w	**455 w**
1598 m	1001 w	531 w	1540 w	**941 s**	389 w
1548 m	964 w	**458 w**	1485 w	909 w	
1504 m	**941 w**		1445 w	820 s	
1434 m	818 w		1362 w	**636 w**	

The product was also characterized by powder X-ray diffraction. Selected diffraction maxima were read from the pattern and they are listed in Table 13.

Table 13: Selected diffraction maxima and d-spacing for **$(DAMT)_2\ ClO_4 \cdot 2H_2O$**.

Position (°2θ)	d-spacing (Å)	Rel. Int. (%)	Position (°2θ)	d-spacing (Å)	Rel. Int. (%)
8.866	9.974	100.00	28.926	3.087	7.40
17.660	5.022	25.13	29.398	3.036	10.95
19.030	4.664	4.79	29.540	3.029	7.58
19.720	4.502	5.08	30.892	2.892	3.96
20.258	4.384	4.75	34.205	2.619	2.25
21.124	4.206	27.19	42.191	2.140	6.49
21.529	4.128	17.66	42.311	2.140	3.71
21.698	4.096	9.46	45.736	1.982	0.93
23.938	3.717	10.81	50.627	1.802	1.28
24.820	3.587	19.29	51.032	1.788	1.58
25.824	3.450	9.72	52.196	1.751	1.19
26.833	3.323	44.06	54.538	1.681	0.81

2,4-diamino-1,3,5-triazonium(1+) chloride – product **DAMT Cl**

This product was obtained from the solutions of **DAMT** and hydrochloric acid in molar ratio 1:1. Chemical formula of this salt is $C_3H_6ClN_5$, relative molecular mass is 147.58. The salt belong to the triclinic system with space group *P*–1 (*a* = 4.8932(3) Å, *b* = 7.3722(3) Å, *c* = 8.9579(5) Å, α = 94.323(3)°, β = 102.427(2)°, γ = 102.921(2)°, *V* = 304.98(3) Å^3).

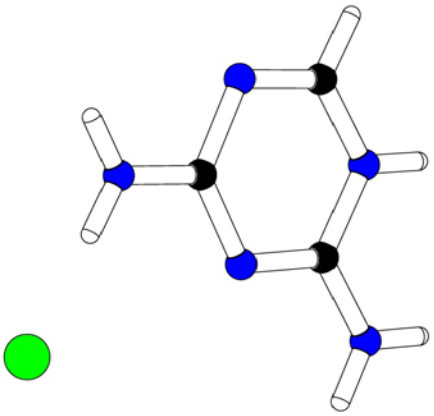

Figure 19: Asymmetric unit of **DAMT Cl** (C – black, N – blue, Cl – green).

The crystal structure contains the chains of cations connected *via* N–H…N hydrogen bonds. There are always two hydrogen bonds between neighboring cations. These chains are interconnected by chloride anion *via* N–H…Cl hydrogen bonds to form a layer as seen in Figure 20.

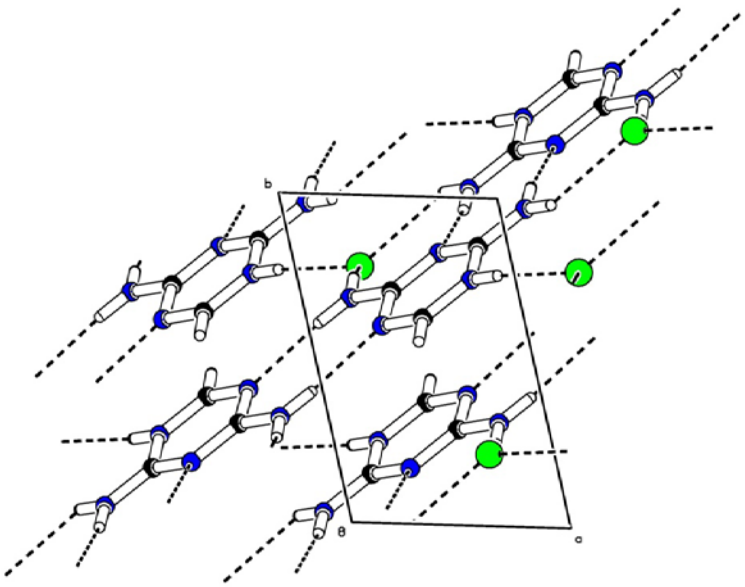

Figure 20: Crystal packing of **DAMT Cl**, view along the crystallographic axis *c*. The dashed lines indicate the hydrogen bonds.

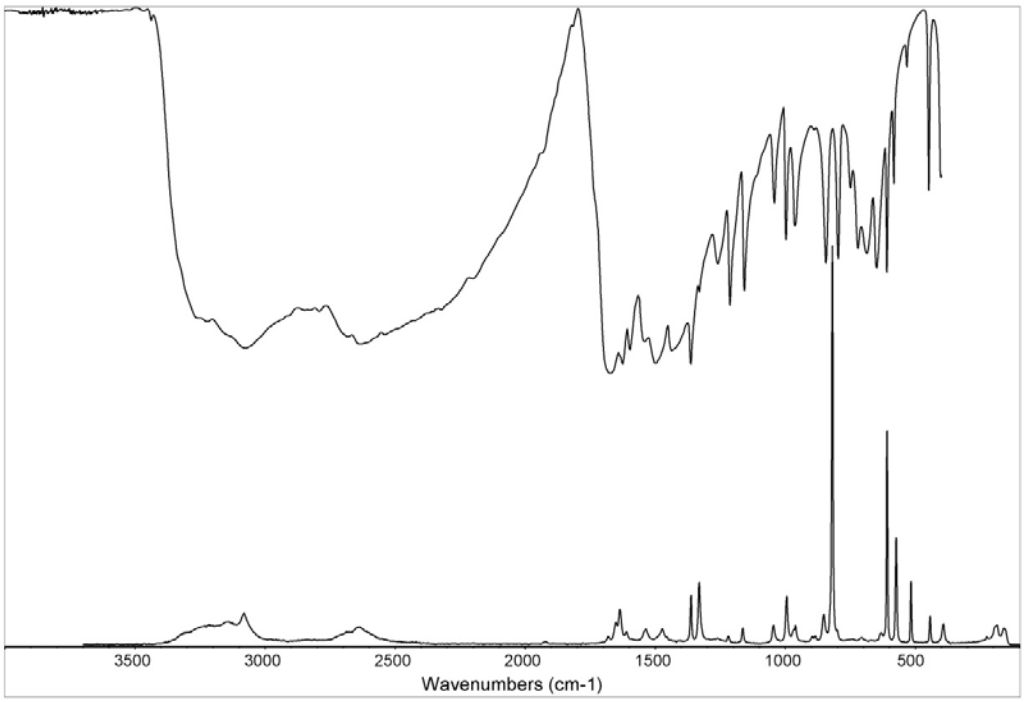

Figure 21: IR (compiled from nujol and fluorolube mulls) and Raman spectra of **DAMT Cl**.

The IR and Raman spectra are depicted in Figure 21. The values of vibrational frequencies were read from the spectra and they are listed in Table 14.

Table 14: Recorded vibrational frequencies of **DAMT Cl**.

IR (cm^{-1})			Raman (cm^{-1})		
3220 m	1364 s	753 w	3081 w	995 w	190 w
3075 m	1330 w	721 m	2640 w	962 w	160 w
2790 m	1260 w	687 m	1636 w	852 w	
2630 m	1213 m	649 m	1540 w	819 s	
1674 s	1158 m	609 m	1470 w	636 w	
1626 s	1042 w	583 w	1362 w	608 m	
1598 m	998 w	532 w	1331 w	574 w	
1545 m	964 w	448 w	1218 w	517 w	
1499 s	844 m		1164 w	443 w	
1438 m	797 m		1046 w	391 w	

The product was also characterized by powder X-ray diffraction. Selected diffraction maxima were read from the pattern and they are listed in Table 15.

Table 15: Selected diffraction maxima and d-spacing for **DAMT Cl**.

Position (°2θ)	d-spacing (Å)	Rel. Int. (%)	Position (°2θ)	d-spacing (Å)	Rel. Int. (%)
10.246	8.633	53.13	30.289	2.951	4.08
15.053	5.886	8.94	31.836	2.811	5.28
22.606	3.933	6.38	32.096	2.789	4.43
24.826	3.586	6.39	34.785	2.579	5.59
25.221	3.531	3.57	45.024	2.014	3.16
25.408	3.506	4.87	49.533	1.840	1.45
26.268	3.393	18.94	52.558	1.741	1.51
27.290	3.268	7.18	54.198	1.692	1.42
28.598	3.121	100.00	59.085	1.562	0.93

6.3 Systems containing DAMT and organic acids

This part contains results of crystallization of 2,4-diamino-1,3,5-triazine with organic acids. The studied systems are presented in Table 16. This chapter describes the structures of salts or co-crystals and also data from all measurements are included.

Table 16: Systems of 2,4-diamino-1,3,5-triazine and organic acids.

Acid	Ratio	Product	Acid	Ratio	Product
formic	1:1	**DAMT**	adipic	1:1	**DAMT H_2adp**
	1:2	**DAMT**		1:2	**DAMT H_2adp**
malonic	1:1	**DAMT Hmalon**	L–malic	1:1	**DAMT**
	1:2	**DAMT Hmalon**		1:2	**DAMT HLmal · H_2O**
succinic	1:1	**DAMT H_2suc · H_2O**	L–tartaric	1:1	**$(DAMT)_2$ Ltar**
	1:2	**DAMT Hsuc**		1:2	**$(DAMT)_2$ Ltar**
glutaric	1:1	**DAMT + DAMT H_2glu**			
	1:2	**DAMT H_2glu**			

2,4-diamino-1,3,5-triazine and formic acid

The only product of this crystallization was the re-crystallized starting base therefore this system was not further studied.

2,4-diamino-1,3,5-triazinium(1+) hydrogen malonate – product **DAMT Hmalon**

This salt was obtained from the solutions of **DAMT** and malonic acid in molar ratios 1:1 and 1:2 (see Table 16). Based on single crystal X-ray analysis it was found that chemical formula of this salt is $C_6H_9N_5O_4$, relative molecular mass is 215.18. Crystal system is triclinic with space group *P*–1 (a = 5.0844(3) Å, b = 7.0995(4) Å, c = 12.8523(8) Å, α = 97.165(3)°, β = 97.552(2)°, γ = 105.765(2)°, V = 436.29(5) Å^3).

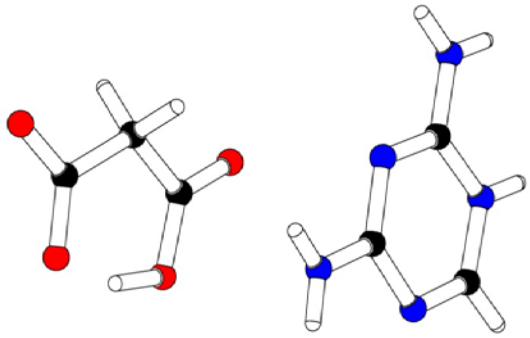

Figure 22: Asymmetric unit of **DAMT Hmalon**. (C – black, N – blue, O – red).

The crystal structure contains chains of the cations where **DAMT(1+)** cations are connected by two N–H…N hydrogen bonds. These chains are interconnected by hydrogen malonate anions *via* N–H…O hydrogen bonds to form layers. Additionally, hydrogen malonates exhibit an intramolecular hydrogen interaction O–H…O as seen in Figure 23.

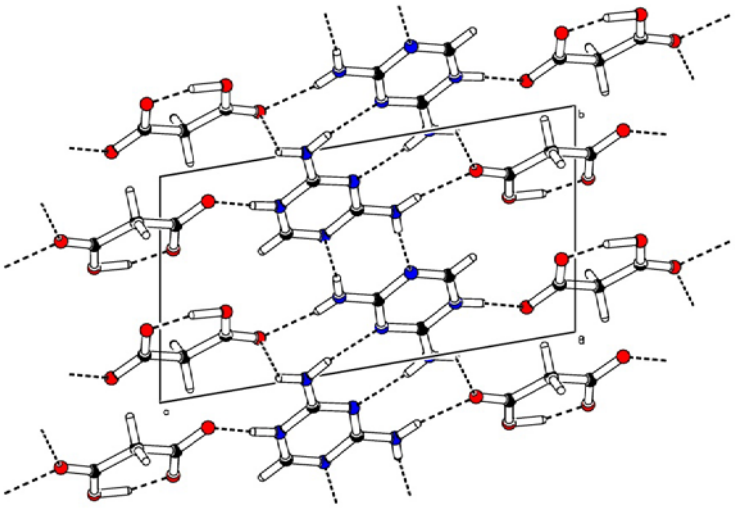

Figure 23: Crystal packing of **DAMT Hmalon**, view along the crystallographic axis *a*. The dashed lines indicate the hydrogen bonds.

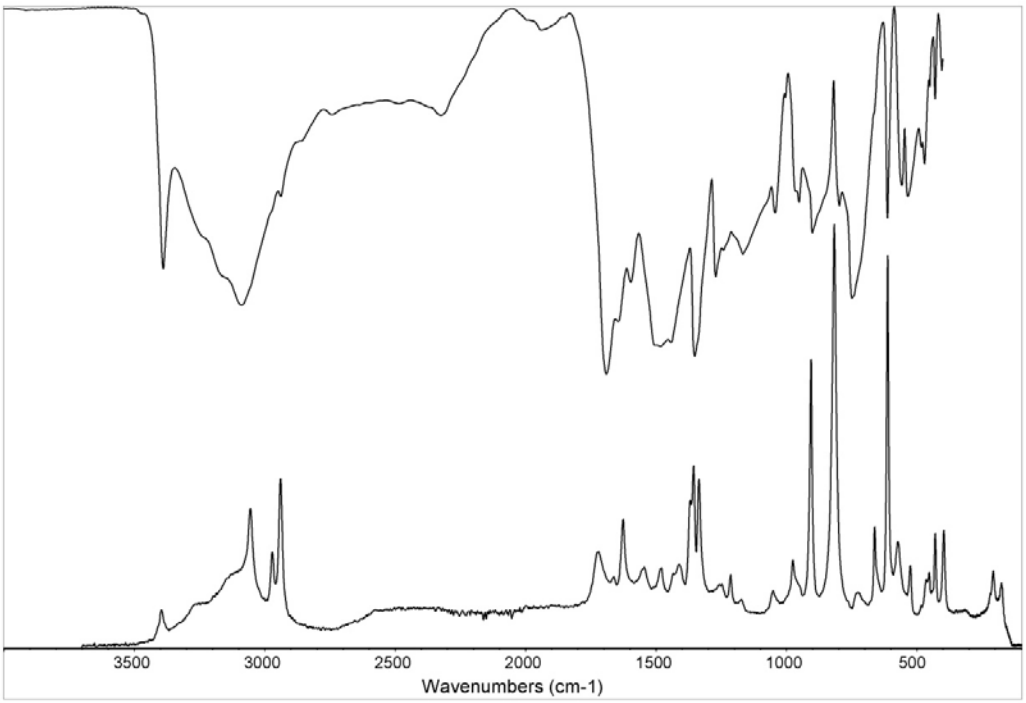

Figure 24: IR (compiled from nujol and fluorolube mulls) and Raman spectra of **DAMT Hmalon**.

The IR and Raman spectra are depicted in Figure 24. The values of vibrational frequencies were read from the spectra and they are listed in Table 17.

Table 17: Recorded vibrational frequencies of **DAMT Hmalon**.

IR (cm^{-1})		Raman (cm^{-1})		
3389 m	1044 w	3396 w	1336 m	573 w
3090 m	952 w	3055 m	1254 w	525 w
2937 w	901 w	2971 w	1214 w	453 w
2330 w	800 w	2939 m	1172 w	430 w
1691 s	749 m	1721 w	1054 w	400 w
1645 m	613 w	1664 w	975 w	209 w
1597 m	558 w	1626 w	906 s	179 w
1480 m	535 w	1546 w	817 s	
1352 s	471 w	1480 w	727 w	
1272 m	430 w	1414 w	662 w	
1168 m		1356 m	612 s	

The product was also characterized by powder X-ray diffraction. Selected diffraction maxima were read from the pattern and they are listed in Table 18.

Table 18: Selected diffraction maxima and d-spacing for **DAMT Hmalon**.

Position (°2θ)	d-spacing (Å)	Rel. Int. (%)	Position (°2θ)	d-spacing (Å)	Rel. Int. (%)
13.783	6.425	0.36	26.156	3.413	2.32
14.112	6.276	0.66	26.992	3.301	2.84
17.617	5.034	1.22	28.161	3.166	100.00
18.494	4.794	2.79	31.067	2.876	0.21
18.564	4.788	2.36	35.652	2.516	0.25
20.772	4.273	0.69	40.425	2.229	0.20
23.081	3.850	0.93	52.312	1.747	0.18
25.412	3.502	0.55	54.592	1.680	0.07
26.085	3.413	2.41	58.107	1.586	0.82

2,4-diamino-1,3,5-triazine – succinic acid (1/1) monohydrate – product **DAMT H_2suc · H_2O**

This adduct was obtained from the starting solutions of **DAMT** and succinic acid in molar ratio 1:1. Chemical formula of this salt is $C_8H_{10}N_3O_4$, relative molecular mass is 212.19. The compound belongs to the triclinic system with space group *P*–1 (*a* = 6.2839(6) Å, *b* = 6.6097(8) Å, *c* = 10.642(1) Å, α = 103.185(4)°, β = 94.312(4)°, γ = 106.620(4)°, *V* = 407.69(7) Å^3).

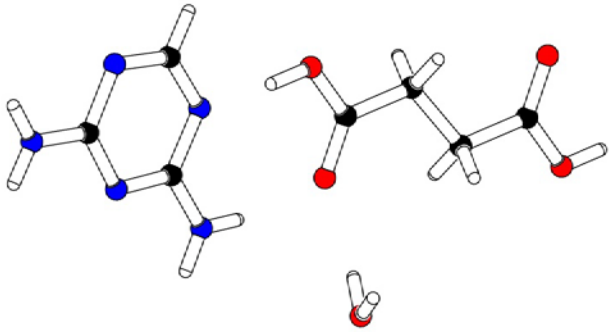

Figure 25: Asymmetric unit of **DAMT H_2suc · H_2O** (C – black, N – blue, O – red).

The structure consists of the molecules of the 2,4-diamino-1,3,5-triazine arranged to centrosymmetric pairs connected *via* two N–H…N hydrogen bonds. NH_2 group of one base is connected with nitrogen atom located in the ring between the two substituted carbon atoms. Molecules of the succinic acid and molecules of water form chains *via* O–H…O hydrogen bonds and they are interconnected with the pairs of base to 3D structure *via* O–H…N hydrogen bonds.

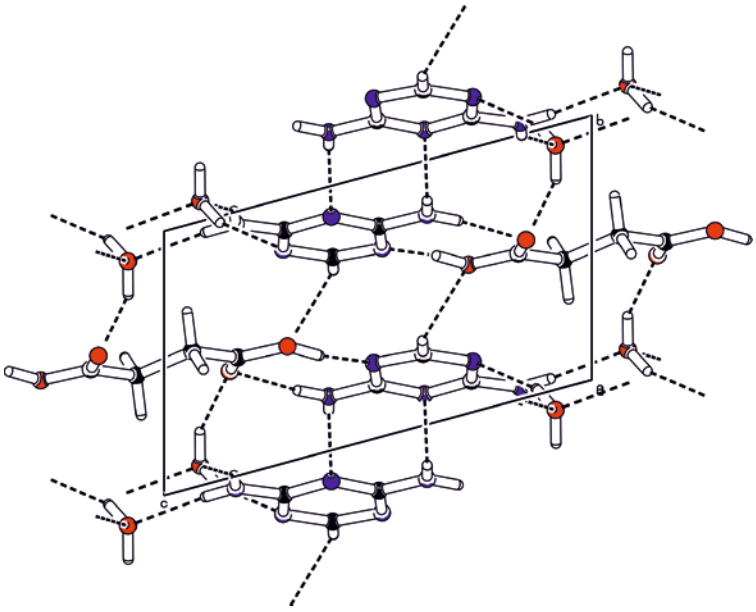

Figure 26: Crystal packing of **DAMT H_2suc · H_2O**, view along the crystallographic axis *a*. The dashed lines indicate the hydrogen bonds.

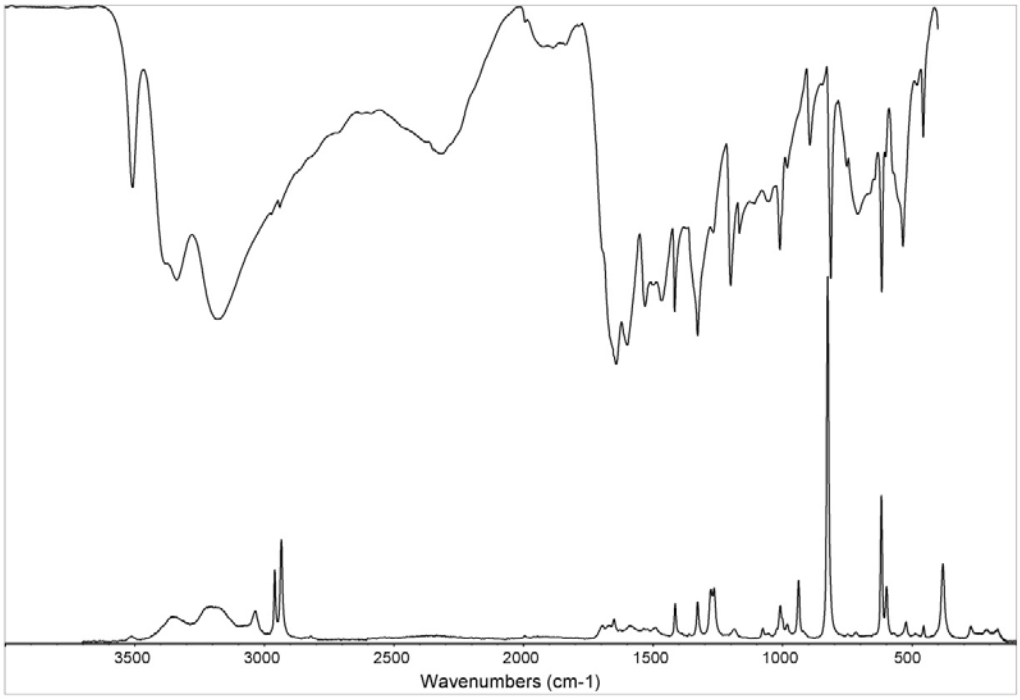

Figure 27: IR (compiled from nujol and fluorolube mulls) and Raman spectra of **DAMT H_2suc · H_2O**.

The IR and Raman spectra are depicted in Figure 27. The values of vibrational frequencies were read from the spectra and they are listed in Table 19.

Table 19: Recorded vibrational frequencies of **DAMT H_2suc · H_2O**.

IR (cm^{-1})			Raman (cm^{-1})		
3509 w	1468 m	983 w	3510 w	1328 w	618 m
3390 m	1417 m	895 w	3350 w	1278 w	599 w
3339 m	1328 m	814 m	3200 w	1264 w	524 w
3181 s	1268 w	753 w	3035 w	1186 w	456 w
2317 w	1201 m	710 w	2960 w	1078 w	380 m
1643 s	1167 w	617 m	2934 m	1009 w	277 w
1601 s	1109 w	535 m	1696 w	983 w	215 w
1531 m	1053 w	457 w	1651 w	938 w	168 w
1501 w	1011 w		1414 w	826 s	

The product was also characterized by powder X-ray diffraction. Selected diffraction maxima were read from the pattern and they are listed in Table 20.

Table 20: Selected diffraction maxima and d-spacing for **DAMT H_2suc · H_2O.**

Position (°2θ)	d-spacing (Å)	Rel. Int. (%)	Position (°2θ)	d-spacing (Å)	Rel. Int. (%)
8.657	10.213	3.21	27.497	3.244	9.92
14.871	5.957	1.37	27.690	3.222	43.66
16.064	5.517	15.32	27.853	3.203	100.00
18.406	4.820	1.35	28.205	3.164	5.87
19.856	4.472	1.11	29.937	2.985	1.22
23.210	3.832	2.27	40.028	2.253	0.32
23.740	3.748	2.01	54.658	1.679	1.51
25.508	3.492	0.84	56.311	1.634	0.33
26.690	3.340	2.14	57.521	1.601	0.30

2,4-diamino-1,3,5-triazinium(1+) hydrogen succinate – product **DAMT Hsuc**

When the molar ratio base/acid was changed to 1:2, the other compound was obtained from the solutions. This compound (**DAMT Hsuc**) was also characterized by vibrational spectroscopy and powder X-ray diffraction. Based on vibrational spectroscopy it is possible to differentiate this salt from the co-crystal **DAMT H_2suc · H_2O**. In the spectrum of **DAMT Hsuc** there are seen vibrational modes of **DAMT(1+)** cation (compared with the spectra of **DAMT Cl**) contrary to the spectra of **DAMT H_2suc · H_2O** where the vibrational modes of uncharged molecule are obvious. Additionally, the manifestations of hydrogen

succinate anion were assigned by the comparison with the organic salts of hydrogen succinate.[27, 28] The IR and Raman spectra of **DAMT Hsuc** are depicted in Figure 28 and values of vibrational frequencies read from the spectra are listed in Table 21.

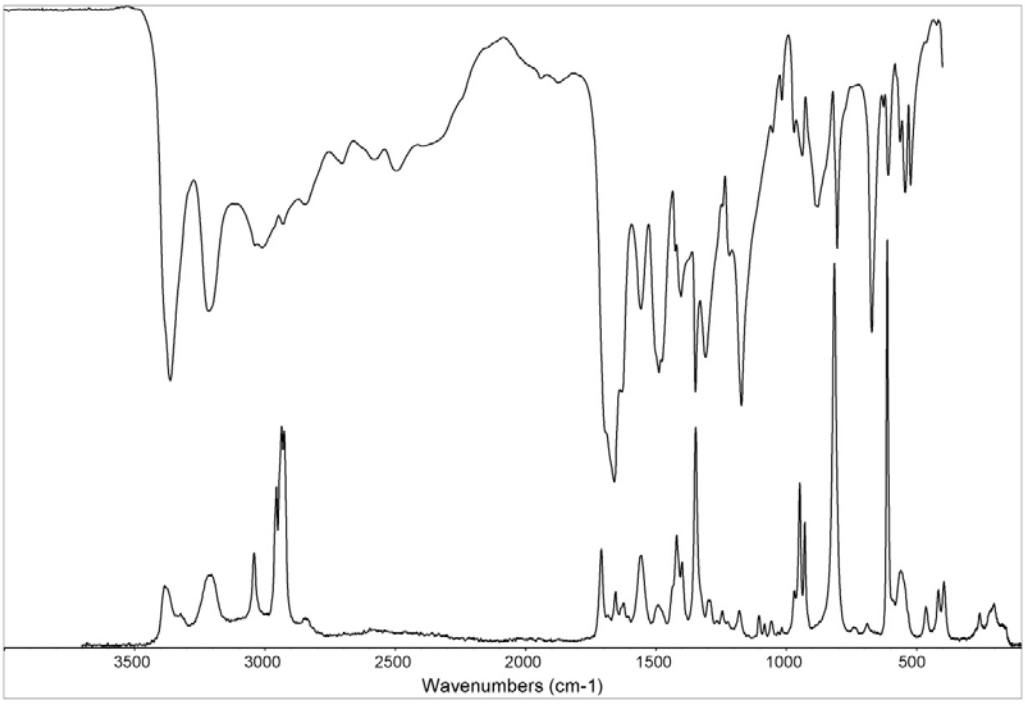

Figure 28: IR (compiled from nujol and fluorolube mulls) and Raman spectra of **DAMT Hsuc**.

Table 21: Recorded vibrational frequencies of **DAMT Hsuc**.

IR (cm^{-1})			Raman (cm^{-1})		
3364 m	1489 m	880 w	3385 w	1490 w	816 s
3215 w	1404 w	805 w	3321 w	1421 w	692 w
3010 w	1349 m	672 w	3205 w	1400 w	613 s
2930 w	1310 m	609 w	3042 w	1348 m	560 w
2840 w	1224 w	544 w	2956 w	1299 w	465 w
2700 w	1218 w	524 w	2936 m	1245 w	416 w
2580 w	1173 m		2926 m	1180 w	394 w
2500 w	1050 w		1709 w	1105 w	259 w
1660 s	1018 w		1655 w	1057 w	203 w
1633 m	974 w		1628 w	948 m	
1558 w	940 w		1557 w	929 w	

The product was also characterized by powder X-ray diffraction. Selected diffraction maxima were read from the pattern and they are listed in Table 22.

Table 22: Selected diffraction maxima and d-spacing for **DAMT Hsuc.**

Position (°2θ)	d-spacing (Å)	Rel. Int. (%)	Position (°2θ)	d-spacing (Å)	Rel. Int. (%)
7.220	12.244	0.06	22.563	3.941	0.23
13.358	6.628	0.13	24.293	3.664	0.31
13.877	6.382	0.19	25.776	3.456	1.99
16.924	5.239	0.08	26.890	3.316	100.00
17.520	5.062	0.27	55.371	1.658	1.08
21.476	4.138	0.25	55.527	1.658	0.59

2,4-diamino-1,3,5-triazinie – glutaric acid (1/1) – product **(DAMT H_2glu)**

The adduct **DAMT H_2glu** crystallizes from the molar ratio base/acid 1:2. Chemical formula of this compound is $C_8H_{13}N_5O_4$, relative molecular mass is 243.23. The product is non-centrosymmetric, crystal system is orthorhombic, space group *Pma*2 (*a* = 27.330(2) Å, *b* = 3.9465(3) Å, *c* = 4.9803(3) Å, *V* = 537.15(7) Å^3).

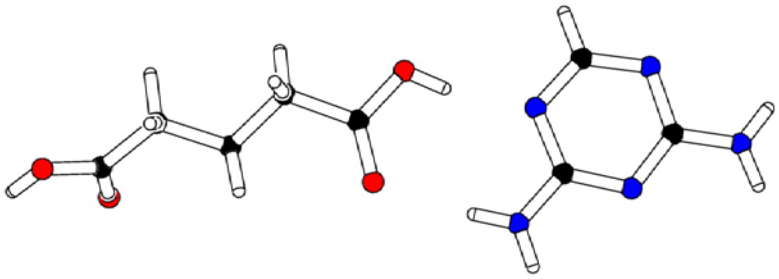

Figure 29: Asymmetric unit of **DAMT H_2glu** (C – black, N – blue, O – red).

The crystal structure of this adduct consists of molecules of **DAMT** alternating with molecules of glutaric acid. Each molecule of the organic base is surrounded by four molecules of glutaric acid. Two of them are connected with the base *via* O–H…N and N–H…O hydrogen bonds and the rest of them are connected only *via* N–H…O hydrogen bond (see Figure 30). Molecule of **DAMT** lies in the mirror plane and molecules of glutaric acid are parallel with C_2 axis. The molecules of **DAMT** are not interconnected *via* hydrogen bonds as well as the molecules of glutaric acids themselves.

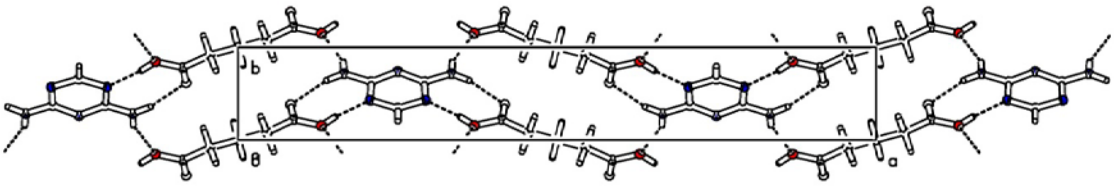

Figure 30: Crystal packing of **DAMT H_2glu**, along the crystallographic axis *c*. The dashed lines indicate the hydrogen bonds.

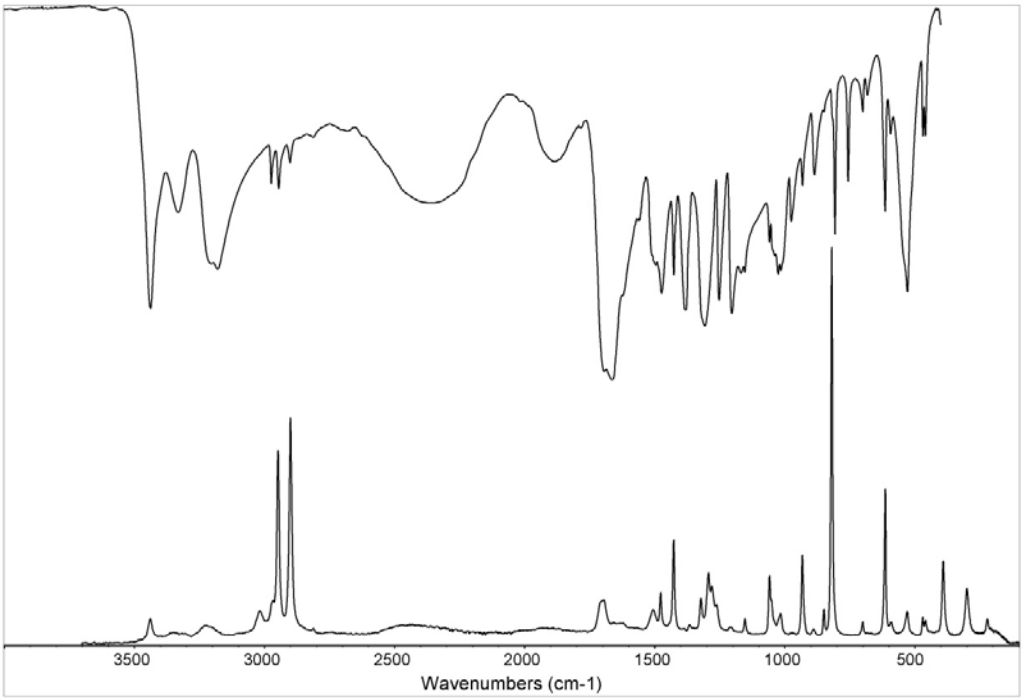

Figure 31: IR (compiled from nujol and fluorolube mulls) and Raman spectra of **DAMT H_2glu**.

The IR and Raman spectra are depicted in Figure 31. The values of vibrational frequencies were read from the spectra and they are listed in Table 23.

Table 23: Recorded vibrational frequencies of **DAMT H_2glu**.

IR (cm^{-1})			Raman (cm^{-1})	
3438 m	1427 m	756 w	3439 w	1058 w
3330 w	1380 m	701 w	3220 w	1016 w
3180 m	1308 m	683 w	3018 w	932 w
2974 w	1253 m	614 w	2948 m	850 w
2945 w	1204 m	591 w	2900 m	819 s
2902 w	1171 m	529 m	1695 w	704 w
2350 w	1059 w	469 w	1505 w	614 m
1890 w	1026 m	460 w	1477 w	530 w
1698 s	975 w		1427 w	470 w
1665 s	932 w		1322 w	391 w
1500 m	886 w		1293 w	300 w
1474 m	807 w		1154 w	224 w

The product was also characterized by powder X-ray diffraction. Selected diffraction maxima were read from the pattern and they are listed in Table 24.

Table 24: Selected diffraction maxima and d-spacing for **DAMT H_2glu**.

Position (°2θ)	d-spacing (Å)	Rel. Int. (%)	Position (°2θ)	d-spacing (Å)	Rel. Int. (%)
6.609	13.374	36.42	28.738	3.107	100.00
17.942	4.944	67.65	29.301	3.048	5.65
19.059	4.657	67.49	31.827	2.809	3.89
19.603	4.529	9.32	31.950	2.801	5.36
22.115	4.020	5.78	34.748	2.579	3.15
22.364	3.975	4.30	37.561	2.393	5.30
23.023	3.863	43.70	41.437	2.177	4.33
24.199	3.678	36.11	48.868	1.862	2.16
26.633	3.347	8.12	49.574	1.837	1.57
27.523	3.241	7.17	49.809	1.829	3.27
28.527	3.129	49.57	59.075	1.563	1.67

2,4-diamino-1,3,5-triazine – adipic acid (1/1) – product **DAMT H_2adp**

This adduct crystallizes from the solutions of **DAMT** and adipic acid in molar ratio 1:1 as well as 1:2. Chemical formula of this compound is $C_{17}H_{23}N_{12}O_7$, relative molecular

mass is 507.47. This adduct crystallizes in orthorhombic system with space group *Pnma* (a = 24.4809(9) Å, b = 29.703(1) Å, c = 6.4232(2) Å, V = 4670.6(3) Å^3).

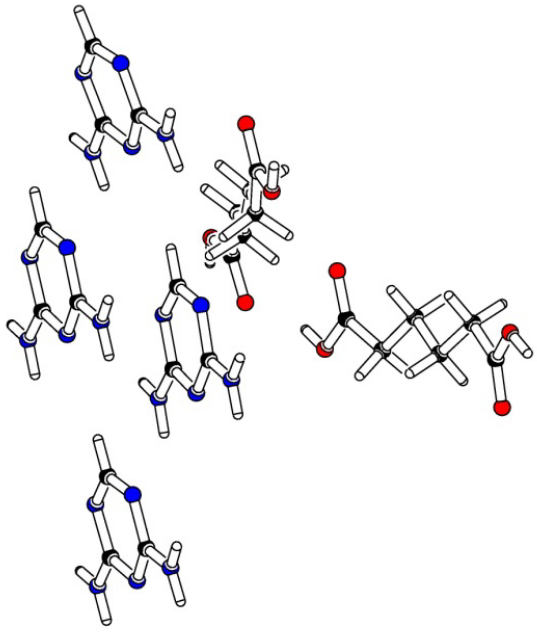

Figure 32: Asymmetric unit of **DAMT H_2adp**. (C – black, N – blue, O – red).

The crystal structure consists of the alternating molecules of **DAMT** and adipic acid connected *via* O–H…N hydrogen bonds. There are no hydrogen bonds among the molecules of organic base themselves. This 3D network of crystal packing is depicted in Figure 33.

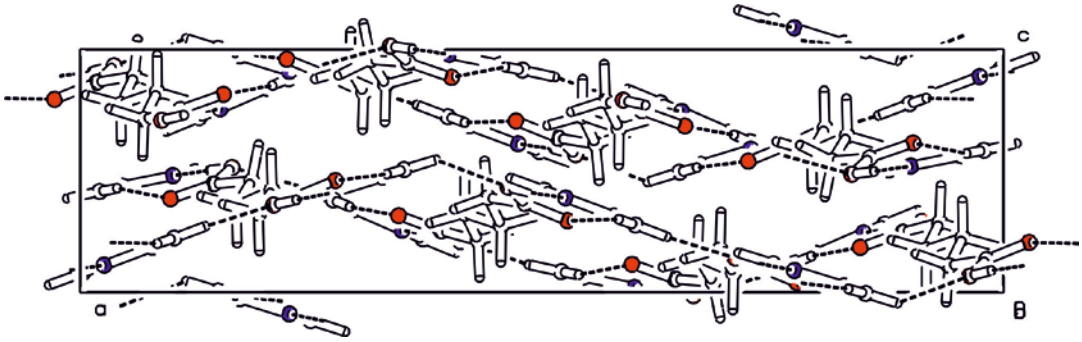

Figure 33: Crystal packing of **DAMT H_2adp**, view along the crystallographic axis *b*. The dashed lines indicate the hydrogen bonds.

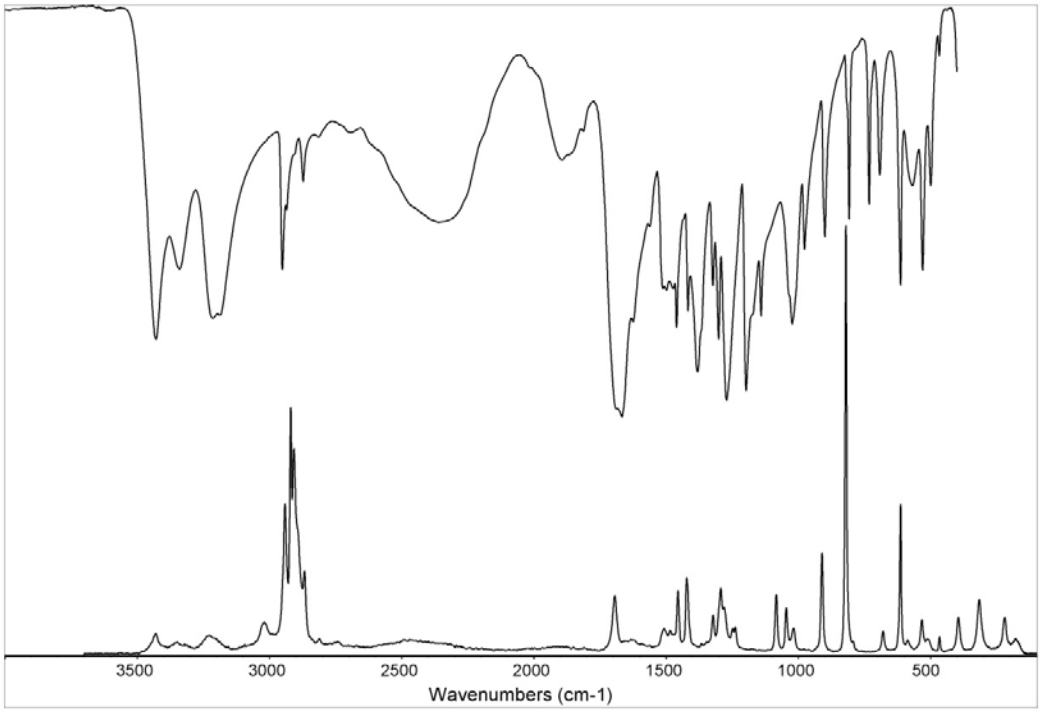

Figure 34: IR (compiled from nujol and fluorolube mulls) and Raman spectra of **DAMT H_2adp**.

The IR and Raman spectra are depicted in Figure 34. The values of vibrational frequencies were read from the spectra and they are listed in Table 25.

Table 25: Recorded vibrational frequencies of **DAMT H_2adp**.

IR (cm^{-1})			Raman (cm^{-1})		
3430 m	1513 w	977 w	3431 w	1294 w	465 w
3341 w	1498 w	900 w	3225 w	1239 w	396 w
3215 m	1461 m	808 w	3020 w	1084 w	316 w
3252 w	1418 w	733 w	2941 m	1046 w	219 w
2873 w	1382 s	692 w	2919 m	1019 w	175 w
2360 w	1323 w	614 m	2907 m	911 m	
1890 w	1302 m	570 w	2868 w	820 s	
1692 s	1272 s	530 m	1695 w	680 w	
1667 s	1198 s	500 w	1507 w	613 m	
1627 m	1141 m	468 w	1455 w	586 w	
1563 w	1024 m		1323 w	533 w	

The product was also characterized by powder X-ray diffraction. Selected diffraction maxima were read from the pattern and they are listed in Table 26.

Table 26: Selected diffraction maxima and d-spacing for **DAMT H_2adp.**

Position (°2θ)	d-spacing (Å)	Rel. Int. (%)	Position (°2θ)	d-spacing (Å)	Rel. Int. (%)
5.975	14.792	33.98	27.457	3.249	82.31
17.571	5.047	5.82	27.620	3.230	79.15
17.922	4.949	8.06	27.912	3.197	80.46
18.349	4.835	7.54	28.063	3.180	100.00
18.814	4.717	8.96	28.336	3.150	64.14
20.687	4.294	6.48	29.499	3.028	3.92
21.746	4.087	3.11	42.044	2.149	2.06
22.635	3.928	3.49	57.685	1.597	1.21
23.609	3.769	3.60			

2,4-diamino-1,3,5-triazinium(1+) hydrogen L–malate monohydrate – product **DAMT HLmal · H_2O**

The salt was obtained from the solution of **DAMT** and L–malic acid in molar ratio 1:2. Chemical formula of this salt is $C_{10}H_{20}N_5O_6$, relative molecular mass is 306.31. The product is non-centrosymmetric, crystal system is triclinic with space group *P*1 (a = 12.0388(3) Å, b = 17.9611(4) Å, c = 26.5612(6) Å, α = 83.420(1)°, β = 89.887(1)°, γ = 80.053(1)°, V = 5618.8(2) Å^3). The structure consists of regularly alternating parallel fragments of cations and anions. This crystal structure is very complicated with disordered atoms. Additionally, one unit cell contains too many asymmetric units and it was not possible to find and refine the hydrogen atoms on the Fourier map.

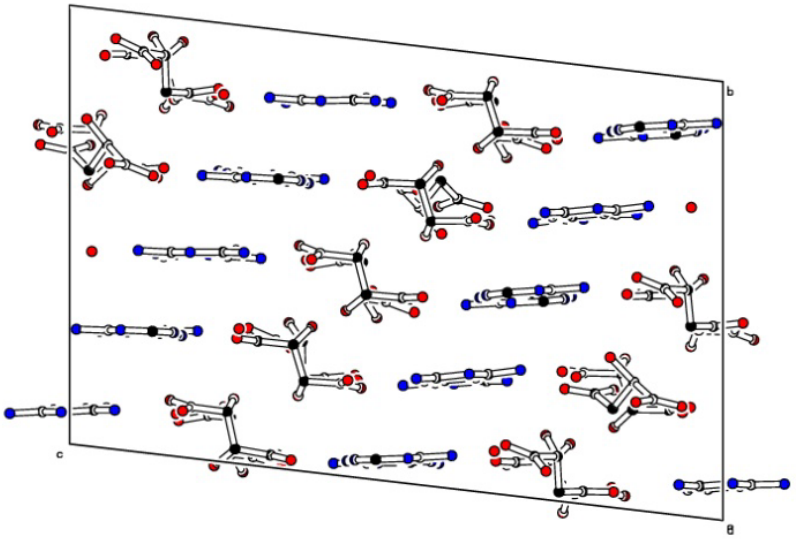

Figure 35: Asymmetric unit and crystal packing of **DAMT HLmal · H_2O**, view along the crystallographic axis *a*. Hydrogen atoms are not depicted (C –black, N – blue, O – red).

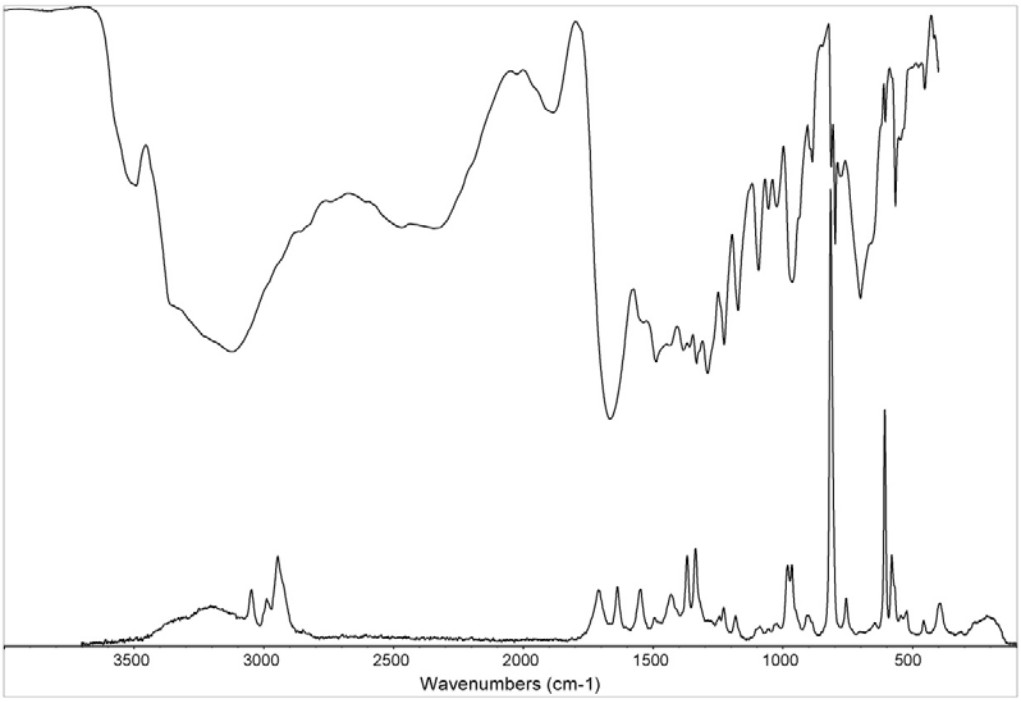

Figure 36: IR (compiled from nujol and fluorolube mulls) and Raman spectra of **DAMT HLmal · H_2O**.

The IR and Raman spectra are depicted in Figure 36. The values of vibrational frequencies were read from the spectra and they are listed in Table 27.

Table 27: Recorded vibrational frequencies of **DAMT HLmal · H_2O**.

IR (cm^{-1})			Raman (cm^{-1})		
3490 w	1333 m	798 m	3048 w	1245 w	607 m
3120 m	1291 m	774 w	2992 w	1228 w	580 w
2350 w	1226 m	702 m	2946 w	1183 w	524 w
1888 w	1173 m	656 m	1711 w	1089 w	459 w
1667 s	1094 m	605 w	1638 w	1030 w	396 w
1542 m	1056 w	566 m	1548 w	983 w	210 w
1488 m	1024 w	544 w	1496 w	965 w	
1436 m	964 m	453 w	1432 w	907 w	
1384 m	887 w		1396 w	816 s	
1360 m	814 w		1337 w	756 w	

The product was also characterized by powder X-ray diffraction. Selected diffraction maxima were read from the pattern and they are listed in Table 28.

Table 28: Selected diffraction maxima and d-spacing for **DAMT HLmal · H_2O**.

Position (°2θ)	d-spacing (Å)	Rel. Int. (%)	Position (°2θ)	d-spacing (Å)	Rel. Int. (%)
5.089	17.365	1.68	23.700	3.754	5.95
10.112	8.748	0.97	24.931	3.572	100.00
15.205	5.827	6.89	27.441	3.250	3.73
15.771	5.619	10.81	28.134	3.172	2.09
18.858	4.706	4.83	29.999	2.979	32.56
19.456	4.563	10.08	34.059	2.632	4.59
20.365	4.361	11.48	38.159	2.358	2.39
21.275	4.176	14.37	40.838	2.208	1.79
21.815	4.074	4.35			

bis(2,4-diamino-1,3,5-triazinium(1+)) L–tartrate – product **$(DAMT)_2$ Ltar**

The crystallization of base and L–tartaric acid yields into the salt in molar ratio of **DAMT**/acid 1:1 as well as 1:2. Chemical formula of the formed salt is C_4HNO, relative molecular mass is 79.06. The product is non-centrosymmetric, crystal system is monoclinic with space group $P2_1$ (a = 4.9255(3) Å, b = 11.3986(7) Å, c = 13.5163(7) Å, β = 100.497(2)°, V = 746.16(8) $Å^3$).

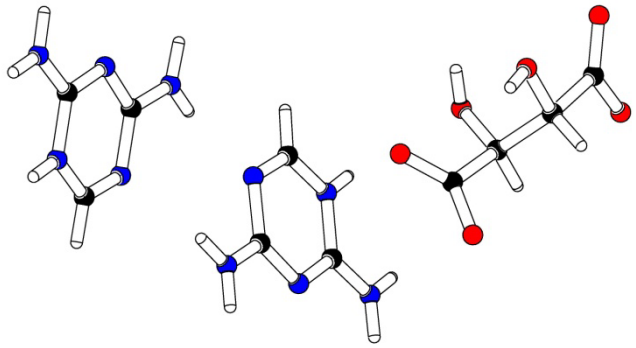

Figure 37: Asymmetric unit of **$(DAMT)_2$ Ltar** (C – black, N – blue, O – red).

The structure consists of **DAMT(1+)** cations and L–tartrate anions. Two **DAMT(1+)** cations are connected *via* N–H…N hydrogen bonds to the pairs. These pairs of **DAMT(1+)** cations are connected with the chains of L–tartrate anions to form 3D structure *via* N–H…O hydrogen bonds. The crystal arrangement is depicted in the Figure 38.

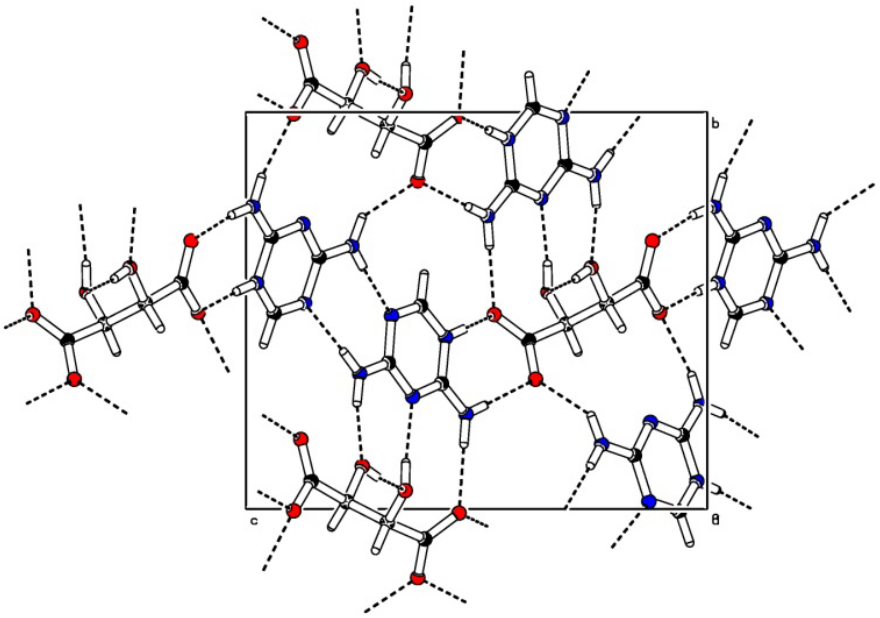

Figure 38: Crystal packing of **(DAMT)$_2$ Ltar**, view along the crystallographic axis *a*. The dashed lines indicate the hydrogen bonds.

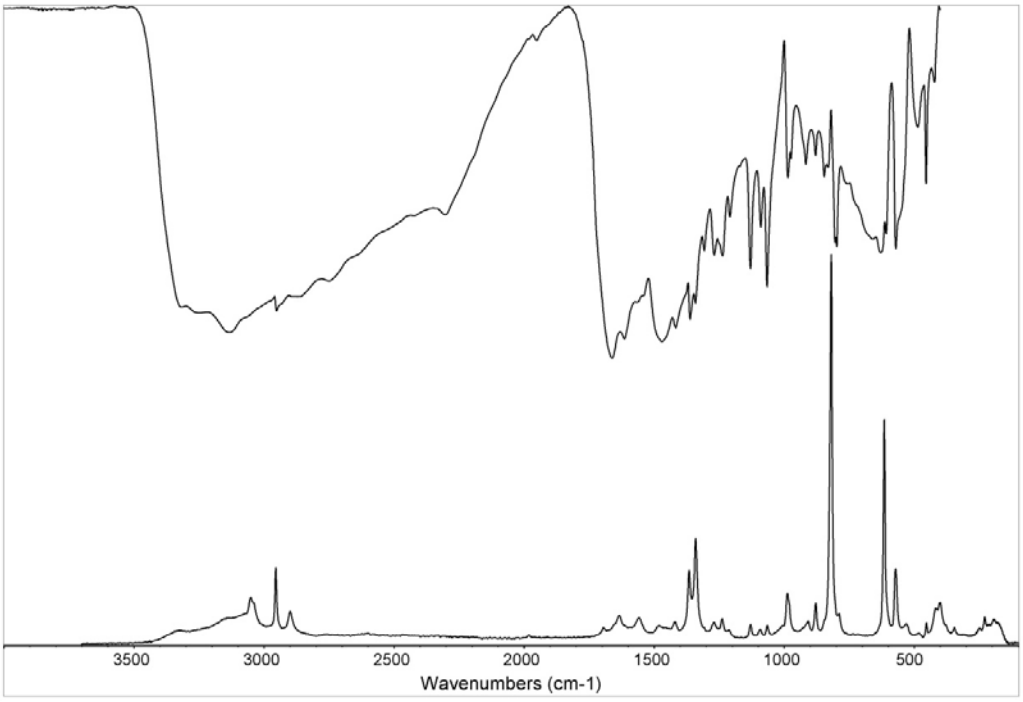

Figure 39: IR (compiled from nujol and fluorolube mulls) and Raman spectra of **(DAMT)$_2$ Ltar**.

The IR and Raman spectra are depicted in Figure 39. The values of vibrational frequencies were read from the spectra and they are listed in Table 29.

Table 29: Recorded vibrational frequencies of **$(DAMT)_2$ Ltar**.

IR (cm^{-1})			Raman (cm^{-1})		
3320 m	1418 s	917 w	3050 w	1092 w	400 w
3250 m	1362 m	880 w	2955 w	1066 w	344 w
3135 s	1341 m	847 w	2900 w	988 w	230 w
2952 m	1308 m	798 m	1634 w	910 w	180 w
2860 m	1269 m	630 m	1558 w	879 w	
2745 m	1237 m	606 m	1422 w	819 s	
2305 w	1209 w	571 m	1366 w	789 w	
1662 s	1130 m	485 w	1340 w	615 m	
1615 s	1090 w	455 w	1272 w	572 w	
1566 m	1066 m	424 w	1237 w	530 w	
1470 s	986 w		1131 w	453 w	

The product was also characterized by powder X-ray diffraction. Selected diffraction maxima were read from the pattern and they are listed in Table 30.

Table 30: Selected diffraction maxima and d-spacing for **$(DAMT)_2$ Ltar.**

Position (°2θ)	d-spacing (Å)	Rel. Int. (%)	Position (°2θ)	d-spacing (Å)	Rel. Int. (%)
10.250	8.630	19.42	25.640	3.474	69.62
15.398	5.755	35.32	29.000	3.079	30.04
15.531	5.703	39.65	29.408	3.037	85.18
16.903	5.246	100.00	31.246	2.863	9.40
18.316	4.844	13.46	34.074	2.631	7.48
19.817	4.480	9.14	36.302	2.475	7.63
20.491	4.334	16.44	38.852	2.318	4.26
21.919	4.055	50.17	48.129	1.891	1.38
24.046	3.701	15.19	50.570	1.805	2.42
24.290	3.664	15.45	55.750	1.649	1.47
25.370	3.511	12.11	57.606	1.600	1.10

6.4 Quantum – chemical calculations

6.4.1 2,4-diamino-1,3,5-triazine

Quantum – chemical calculations were used to find optimal geometry of **DAMT** molecule in vacuum (Figure 40). Energy of this optimized molecule equals to –391.2407 Hartree and it belongs to C_1 point group. The results of optimized geometry (bond lengths and angles) are listed in Table 33 where the calculated values are compared with the values read from determined crystal structures of **(DAMT)$_2$ ClO$_4$ · 2H$_2$O**, **DAMT H$_2$suc · H$_2$O**, **DAMT H$_2$glu**, **DAMT H$_2$adp** and **DAMT**.[18]

.

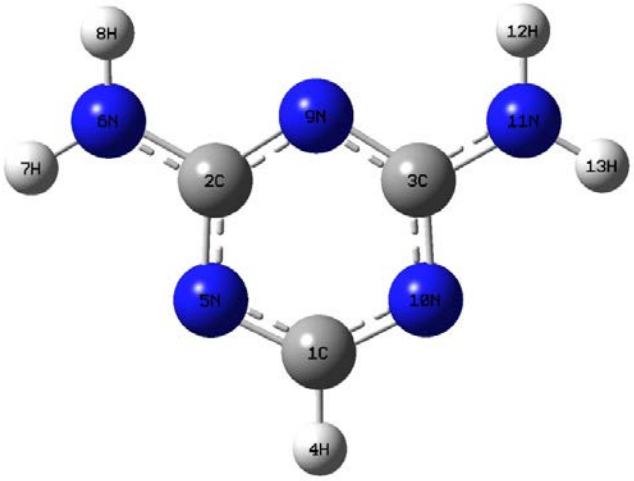

Figure 40: Optimized molecule of **DAMT**.

Further, the values of dipole moment, polarizability and hyperpolarizability components were calculated for this optimized molecule. The values of these physical properties are listed in Table 31 and Table 32. The value of total hyperpolarizability β_{tot} is more than 1.5 times higher than the value of standard molecule of urea (B3LYP/6-311G, $\beta_{tot} = 7.80 \cdot 10^{-31}$ esu) which confirms a potential of 2,4-diamino-1,3,5-triazine in the field of NLO.

Table 31: The values of dipole moment and polarizability for **DAMT**.

Dipole moment (a.u.)	μ_x	μ_y	μ_z
	$-7.49 \cdot 10^{-6}$	$-8.91 \cdot 10^{-1}$	$4.22 \cdot 10^{-7}$
Total dipole moment	$\mu = 2.2638$ Debye		
polarizability (a.u.)	α_{xx}	α_{xy}	α_{yy}
	$1.01 \cdot 10^{2}$	$1.34 \cdot 10^{-5}$	$7.84 \cdot 10^{1}$
	α_{xz}	α_{yz}	α_{zz}
	$-1.05 \cdot 10^{-1}$	$4.42 \cdot 10^{-8}$	$4.26 \cdot 10^{1}$

Table 32: The values of hyperpolarizability components for **DAMT**.

hyperpolarizability (a.u.)	β_{xxx}	β_{xxy}	β_{xyy}	β_{yyy}
	$-2.80 \cdot 10^{-4}$	$2.34 \cdot 10^{2}$	$2.64 \cdot 10^{-4}$	$-6.46 \cdot 10^{1}$
	β_{xxz}	β_{xyz}	β_{yyz}	β_{xzz}
	$-6.50 \cdot 10^{-5}$	-1.57	$-2.89 \cdot 10^{-5}$	$6.02 \cdot 10^{-5}$
	β_{yzz}	β_{zzz}		
	$-2.69 \cdot 10^{1}$	$6.12 \cdot 10^{-6}$		
Total hyperpolarizability	$\beta_{tot} = 1.42 \cdot 10^{2}$ a.u. $= 1.23 \cdot 10^{-30}$ esu			

Table 33: Comparison of theoretical values of bond lengths and angles for **DAMT** molecules and values read from determined crystal structures.

Bond	Calculated (Å)	Crystal structures (Å)	Angle	Calculated (°)	Crystal structures (°)
C1 – N10	1.329	1.320 – 1.328	N5 – C1 – N10	127.20	125.96 – 128.03
N10 – C3	1.350	1.360 – 1.373	H4 – C1 – N10	116.4	116.2 – 117.9
C3 – N9	1.339	1.338 – 1.347	H4 – C1 – N5	116.4	114.1 – 117.0
N9 – C2	1.339	1.332 – 1.349	C1 – N10 – C3	113.64	113.54 – 115.26
C2 – N5	1.350	1.360 – 1.370	N10 – C3 – N9	125.56	124.09 – 124.66
N5 – C1	1.329	1.322 – 1.334	N10 – C3 – N11	116.92	115.87 – 117.51
C1 – H4	1.087	0.93 – 0.97	N9 – C3 – N11	117.52	117.88 – 119.90
C2 – N6	1.353	1.320 – 1.333	C3 – N9 – C2	114.40	115.32 – 115.77
N6 – H7	1.005	0.86 – 0.88	N9 – C2 – N5	125.56	124.07 – 124.60
N6 – H8	1.005	0.86 – 0.90	N9 – C2 – N6	117.51	117.33 – 119.64
C3 – N11	1.353	1.318 – 1.331	N5 – C2 – N6	116.92	116.22 – 118.06
N11 – H12	1.005	0.85 – 0.88	C2 – N5 – C1	113.64	113.46 – 115. 26
N11 – H13	1.005	0.86 – 0.89	C2 – N6 – H7	119.0	118.6 – 120.1
			C2 – N6 – H8	120.1	116.3 – 120.1
			H7 – N6 – H8	120.8	119.9 – 124.3
			C3 – N11 – H12	120.1	118.5 – 120.1
			C3 – N11 – H13	119.0	120.0 – 121.5
			H12 – N11 – H13	120.8	119.7 – 120.1

Moreover, the values of vibrational frequencies and their intensity in IR and Raman spectra were calculated. These values together with complete vibrational assignment of normal modes are listed in Table 34. The comparison of calculated vibrational frequencies with measured IR and Raman spectra of **DAMT** is presented in Figure 41 and Figure 42.

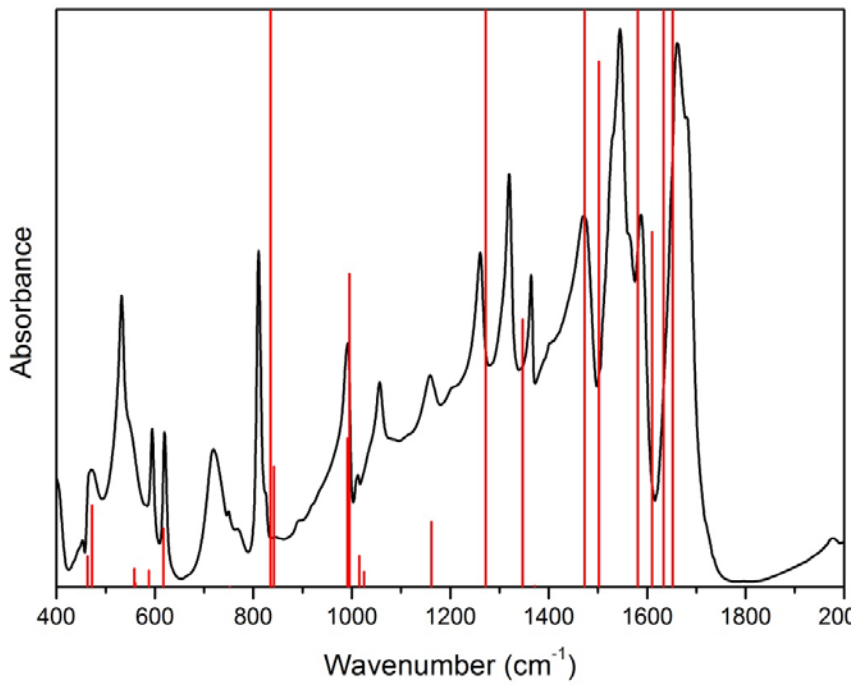

Figure 41: Comparison of experimental IR spectrum and calculated vibrational frequencies (red lines) of **DAMT**.

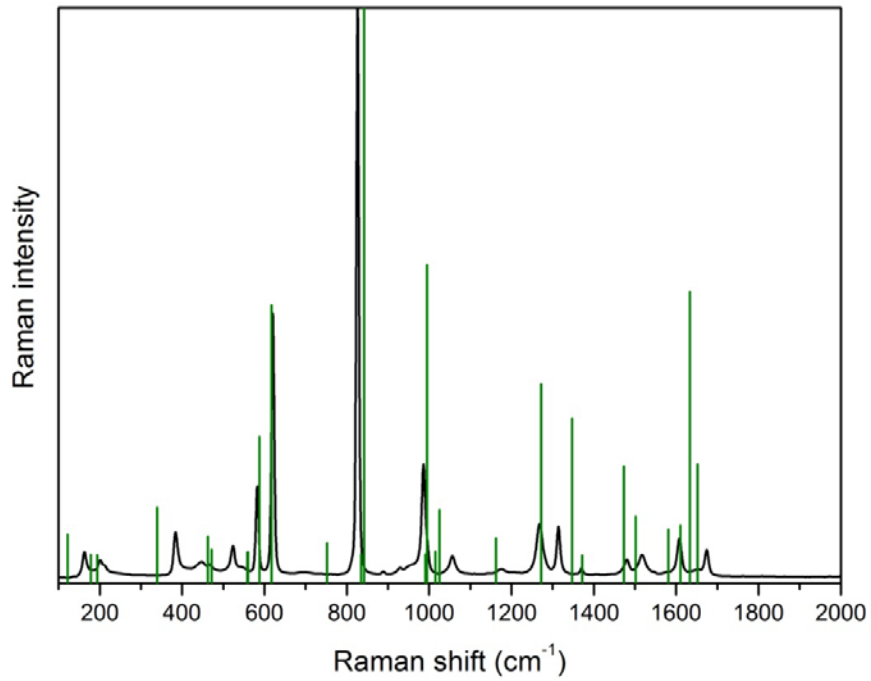

Figure 42: Comparison of experimental Raman spectrum and calculated vibrational frequencies (green lines) of **DAMT**.

Table 34: Theoretical vibrational frequencies of **DAMT** and their assignment.

No	Wavenumber (cm^{-1})	Relative intensity IR/Raman (%)	Assignment
1	95	0/1	ωNH_2
2	122	32/0	ωNH_2
3	178	0/0	γNH, γCNC, γNCN
4	194	4/0	ωNH_2, γCNC
5	339	1/1	ρNH_2
6	463	0/0	γCH, γNCN
7	472	0/0	ρNH_2, δCH
8	558	0/0	τNH_2
9	560	0/0	τNH_2
10	588	0/1	δCNC, δNCN
11	617	0/3	δCNC, δNCN
12	752	0/0	$\gamma_{as}RG$
13	835	3/0	$\gamma_{as}RG$
14	842	0/9	ν_sRG, $\nu C–NH_2$
15	991	1/0	ρNH_2, γCH, νCN
16	995	1/3	δ_sRG, δ_sCNC, ρNH_2
17	1015	0/0	γCH
18	1025	0/1	ρNH_2, δCNC
19	1162	0/0	ρNH_2, νCNC
20	1272	2/2	$\nu_{as}CN$, νNCN, ρNH_2, νRG
21	1347	1/2	δNCN, νCH, γNH, δCNC
22	1372	0/0	δCH, $\nu C–NH_2$, δRG
23	1473	24/1	δCH, $\nu C–NH_2$, δNCN, sci NH_2
24	1502	2/0	sci NH_2, $\nu C–NH_2$, δNCN
25	1581	25/0	ν_sCN, δCNC, νRG, δRG, ρNH_2
26	1610	1/0	sci NH_2, νNCN, δCH
27	1633	100/3	sci NH_2, $\nu C–NH_2$, νNCN, νRG, δCH
28	1652	17/1	sci NH_2, $\nu C–NH_2$, δNCN
29	3152	2/43	νCH
30	3617	12/5	ν_sNH_2
31	3619	3/100	ν_sNH_2
32	3753	3/10	$\nu_{as}NH_2$
33	3754	8/27	$\nu_{as}NH_2$

Note: The intensities of the calculated IR and Raman bands are presented on a relative scale from 0 to 100.

6.4.2 2,4-diamino-1,3,5-triazinium(1+) cation

The same calculations as for the uncharged base was performed for **DAMT(1+)** cation. The optimal geometry of this cation is depicted in Figure 43. Energy of this optimized cation equals to –391.6082 Hartree and it belongs to C_1 point group. The results of optimized geometry are listed in Table 37 where the calculated values are compared with the values read from determined crystal structures of **DAMT NO_3**, **$(DAMT)_2$ $SO_4 \cdot H_2O$**, **DAMT H_2PO_3**, **DAMT H_2PO_4**, **$(DAMT)_2$ $ClO_4 \cdot 2H_2O$**, **DAMT Cl**, **DAMT Hmalon** and **$(DAMT)_2$ Ltar**.

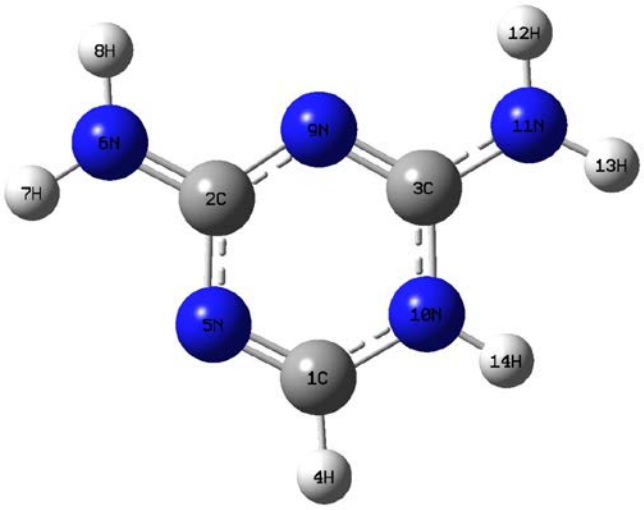

Figure 43: Optimized **DAMT(1+)** cation.

Further, also the values of dipole moment, polarizability and hyperpolarizability components were calculated for this optimized cation. The values of these physical properties are listed in Table 35 and Table 36. The value of total hyperpolarizability β_{tot} is also more than 1.5 times higher than the value of standard molecule of urea (B3LYP/6-311G, $\beta_{tot} = 7.80 \cdot 10^{-31}$ esu) which means that 2,4-diamino-1,3,5-triazinium(1+) cation can be utilized in the field of NLO as well.

Table 35: The values of dipole moment and polarizability for **DAMT(1+)**.

Dipole moment (a.u.)	μ_x	μ_y	μ_z
	1.25	0.20	$1.34 \cdot 10^{-5}$
Total dipole moment	μ = 3.2141 Debye		
Polarizability (a.u.)	α_{xx}	α_{xy}	α_{yy}
	$9.82 \cdot 10^{1}$	3.29	$7.02 \cdot 10^{1}$
	α_{xz}	α_{yz}	α_{zz}
	$5.26 \cdot 10^{-6}$	$-1.28 \cdot 10^{-5}$	$3.64 \cdot 10^{1}$

Table 36: The values of hyperpolarizability for **DAMT(1+)**.

hyperpolarizability (a.u.)	β_{xxx}	β_{xxy}	β_{xyy}	β_{yyy}
	-1.30	$2.15 \cdot 10^{2}$	$1.32 \cdot 10^{1}$	$-6.28 \cdot 10^{1}$
	β_{xxz}	β_{xyz}	β_{yyz}	β_{xzz}
	$-5.12 \cdot 10^{-4}$	$1.96 \cdot 10^{-4}$	$-2.33 \cdot 10^{-5}$	1.62
	β_{yzz}	β_{zzz}		
	$-1.25 \cdot 10^{1}$	$-1.46 \cdot 10^{-4}$		
Total hyperpolarizability	$\beta_{tot} = 1.41 \cdot 10^{2}$ a.u. $= 1.21 \cdot 10^{-30}$ esu			

Table 37: Comparison of theoretical values of bond lengths and angles for **DAMT(1+)** cation and values read from determined crystal structures.

Bond	Calculated (Å)	Crystal structures (Å)	Angle	Calculated (°)	Crystal structures (°)
C1 – N10	1.369	1.338 – 1.350	N5 – C1 – N10	123.16	123.45 – 125.25
N10 – C3	1.380	1.364 – 1.379	H4 – C1 – N10	116.3	117.4 – 118.3
C3 – N9	1.317	1.330 – 1.342	H4 – C1 – N5	120.5	117.4 – 118.6
N9 – C2	1.342	1.334 – 1.355	C1 – N10 – C3	118.66	117.24 – 119.09
C2 – N5	1.378	1.379 – 1.388	C1 – N10 – H14	119.6	120.4 – 121.4
N5 – C1	1.287	1.296 – 1.310	C3 – N10 – H14	121.7	120.5 – 121.3
C1 – H4	1.09	0.950	N10 – C3 – N9	120.38	120.14 – 121.71
C2 – N6	1.323	1.312 – 1.330	N10 – C3 – N11	119.21	117.83 – 118.54
N6 – H7	1.01	0.84 – 0.88	N9 – C3 – N11	120.40	120.14 – 121.61
N6 – H8	1.01	0.84 – 0.93	C3 – N9 – C2	117.27	115.64 – 117.42
C3 – N11	1.332	1.306 – 1.326	N9 – C2 – N5	125.05	124.17 – 125.63
N11 – H12	1.01	0.86 – 0.88	N9 – C2 – N6	118.75	118.21 – 119.63
N11 – H13	1.01	0.86 – 0.88	N5 – C2 – N6	116.20	115.08 – 116.84
N10 – H14	1.01	0.88	C2 – N5 – C1	115.47	113.83 – 115.93
			C2 – N6 – H7	119.7	119.7 – 121.7
			C2 – N6 – H8	120.3	118.8 – 120.9
			H7 – N6 – H8	120.0	117.4 – 121.7
			C3 – N11 – H12	117.9	118.9 – 120.0
			C3 – N11 – H13	123.6	120.0 – 122.0
			H12 – N11 – H13	118.5	119.1 – 120.1

Moreover, the values of vibrational frequencies and their intensity in IR and Raman spectra were calculated. These values together with complete vibrational assignment of

normal modes are listed in Table 38. The comparison of calculated vibrational frequencies with measured IR and Raman spectra of **DAMT Cl** is presented in Figure 44 and Figure 45.

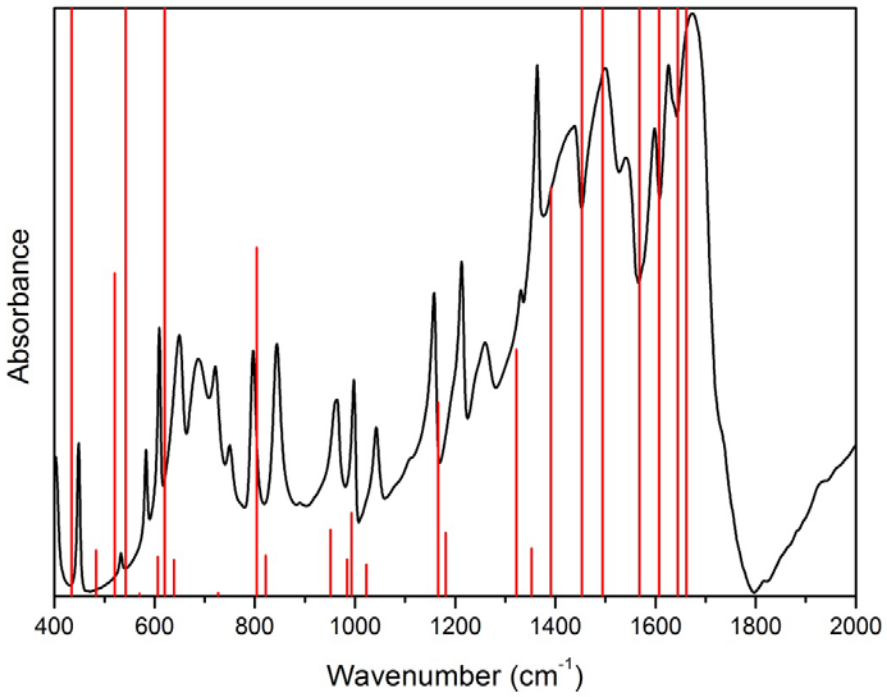

Figure 44: Comparison of experimental IR spectrum and calculated vibrational frequencies (red lines) of **DAMT Cl**.

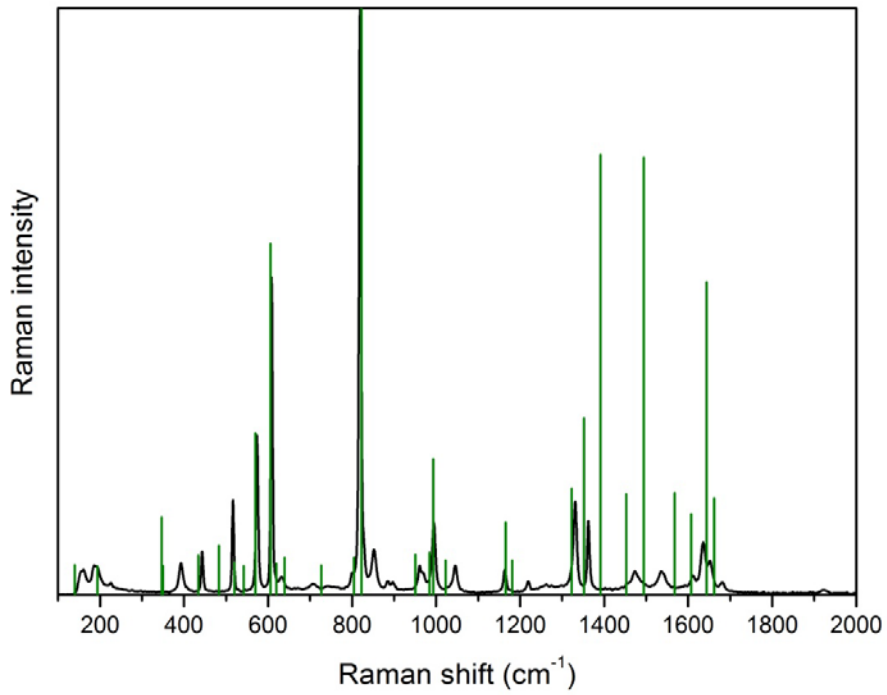

Figure 45: Comparison of experimental Raman spectrum and calculated vibrational frequencies (green lines) of **DAMT Cl**.

Table 38: Theoretical vibrational frequencies of **DAMT(1+)** and their assignment.

No	Wavenumber (cm^{-1})	Relative intensity IR/Raman (%)	Assignment
1	140	2/0	γRG, γNC–NH_2
2	194	1/0	γRG, γNC–NH_2
3	347	1/1	ρNH_2
4	350	15/0	γNH
5	434	9/0	γCH, γ_{as}RG, γNH
6	483	1/0	ρNH_2
7	520	4/0	γNH, ωNH_2
8	542	39/0	ωNH_2, γNH
9	570	0/2	δCNC, δNCN
10	606	0/6	δCNC, δNCN
11	620	8/0	γNH, τNH_2
12	639	0/0	τNH_2
13	727	0/0	γCN_3
14	804	4/0	γ_sRG
15	822	0/16	δ_sRG, νC–NH_2
16	951	1/0	ρNH_2, δCH, ν_{as}CN
17	984	0/0	γCH
18	993	1/2	δCNC, δNCN, ρNH_2
19	1023	0/0	ρNH_2, δCNC
20	1166	2/1	νCN, δNH, δCH, ρ NH_2
21	1181	1/0	ρNH_2, νCNC
22	1369	3/1	δCH, νCNC, δNH
23	1400	1/3	δCH, δNH, νCN, νNCN
24	1440	5/7	νCN, νNCN, δCH, δNH,
25	1504	23/1	νNCN, δCNC, δCH, δNH, ρNH_2
26	1547	17/7	sci NH_2, νNCN, νC–NH_2, δNH
27	1623	10/1	sci NH_2, δNH, νCNC, νNCN
28	1664	61/1	sci NH_2, νC–NH_2, δNH, νCN
29	1702	100/5	sci NH_2, νC–NH_2, δNCN, νCN, δCH, δNH
30	1720	84/1	sci NH_2, νC–NH_2, νNC–NH_2, νCN, δCNC
31	3192	0/47	νCH
32	3572	44/28	$\nu_s$$NH_2$, νNH
33	3577	20/36	νNH, $\nu_s$$NH_2$
34	3587	15/100	νNH, $\nu_s$$NH_2$
35	3699	15/18	$\nu_{as}$$NH_2$
36	3700	18/25	$\nu_{as}$$NH_2$

6.5 SHG measurement

As three of the prepared materials (**DAMT H_2glu, DAMT HLmal · H_2O, $(DAMT)_2$ Ltar**) exhibits non-centrosymmetric arrangement of the crystal structure (*Pma*2, *P*1, $P2_1$) they were examined for the second harmonic generation efficiency. The results are listed in Table 39 as the relative values compared to KDP standard.

Table 39: Results of SHG measurement

Sample	Relative SHG efficiency
DAMT H_2glu	0.74 KDP
DAMT HLmal · H_2O	0.02 KDP
$(DAMT)_2$ Ltar	0.13 KDP

For the most promising sample (**DAMT H_2glu**) also a dependence of the intensity of SHG signal on the power of laser was measured. The experimental data are listed in Table 40. Presented intensity was averaged from seven recorded values while the outlying results were excluded. The values listed in Table 40 were plotted to graph (see Figure 46).

Table 40: Dependence of the SHG intensity on the power of laser for **DAMT H_2glu**.

laser power at 800 nm (mW)	Averaged intensity of SHG at 400 nm (a.u.)	laser power at 800 nm (mW)	Averaged intensity of SHG at 400 nm (a.u.)
250	54	1500	2440
500	239	1750	3363
750	574	2000	4769
1000	1109	2250	5857
1250	1666		

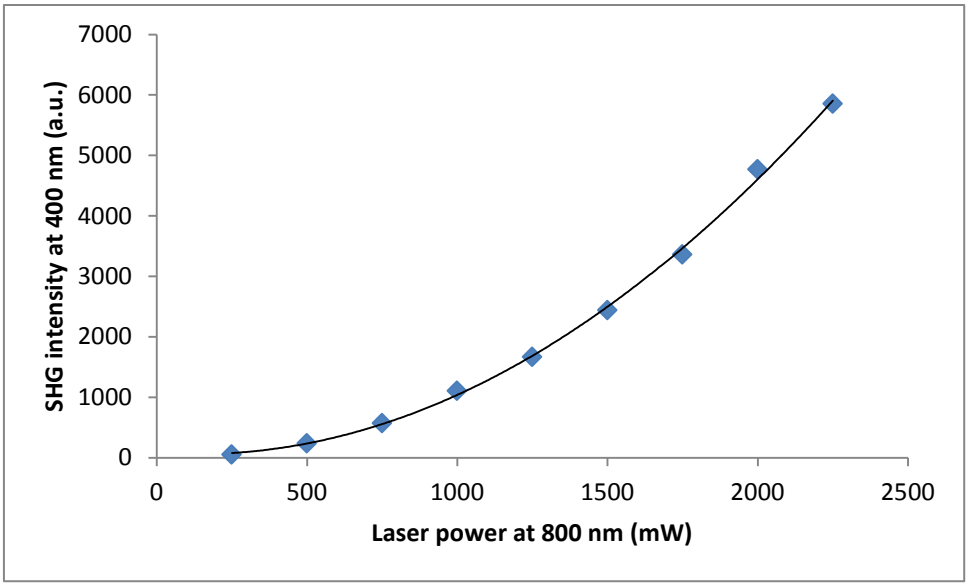

Figure 46: Dependence of the SHG intensity on the power of laser for **DAMT H_2glu**.

7 Discussion

Thirteen new compounds were prepared and characterized within this bachelor's thesis. For twelve of them crystal structure was determined. Among the materials with inorganic acids belong **DAMT NO_3**, **$(DAMT)_2$ $SO_4 \cdot H_2O$**, **DAMT H_2PO_3**, **DAMT H_2PO_4**, **$(DAMT)_2$ $ClO_4 \cdot 2H_2O$** and **DAMT Cl**. All of these six compounds are salts and **$(DAMT)_2$ $ClO_4 \cdot 2H_2O$** contains also an uncharged molecule of **DAMT**. By crystallization with organic acids following compounds were obtained: **DAMT Hmalon**, **DAMT H_2suc $\cdot H_2O$**, **DAMT Hsuc**, **DAMT H_2glu**, **DAMT H_2adp**, **DAMT HLmal $\cdot H_2O$**, **$(DAMT)_2$ Ltar**. Except the **DAMT Hmalon** and **DAMT Hsuc** all compounds obtained from the reaction with achiral organic acids are co-crystals, the next four compounds are salts. The arrangement of **DAMT(1+)** cations or uncharged molecule of **DAMT** differs in the determined structures. Mostly, they are connected *via* N–H…N hydrogen bonds to form chains or pairs excepting **DAMT H_2glu** and **DAMT H_2adp** where the molecules of **DAMT** are not interconnected themselves. In the rest structures four basic types of arrangement were observed. They are depicted in Figure 47 and labeled as type I to type IV. Chains of **DAMT(1+)** cations connected *via* one N–H…N hydrogen bond (type I) were observed in crystal structure of **DAMT NO_3** and **$(DAMT)_2$ $SO_4 \cdot H_2O$** while the crystal structures of **DAMT H_2PO_4**, **$(DAMT)_2$ $ClO_4 \cdot 2H_2O$**, **DAMT Cl** and **DAMT Hmalon** consist of the chains connected *via* two N–H…N hydrogen bonds (type II). The structure of **DAMT H_2PO_3** contains the centrosymmetric pairs of **DAMT(1+)** cations connected via two N–H…N hydrogen bonds where NH_2 group is connected with nitrogen atom from the ring

which is placed between two substituted carbon atoms (type III). The same arrangement of **DAMT** molecules is observed in crystal structure of **DAMT H_2suc · H_2O**. Different type of pairs (type IV) form **DAMT(1+)** cations in crystal structure of **(DAMT)$_2$ Ltar**. Additionally, the crystal packing of **DAMT NO_3**, **DAMT Cl** and **DAMT Hmalon** contains layers while the others form 3D networks.

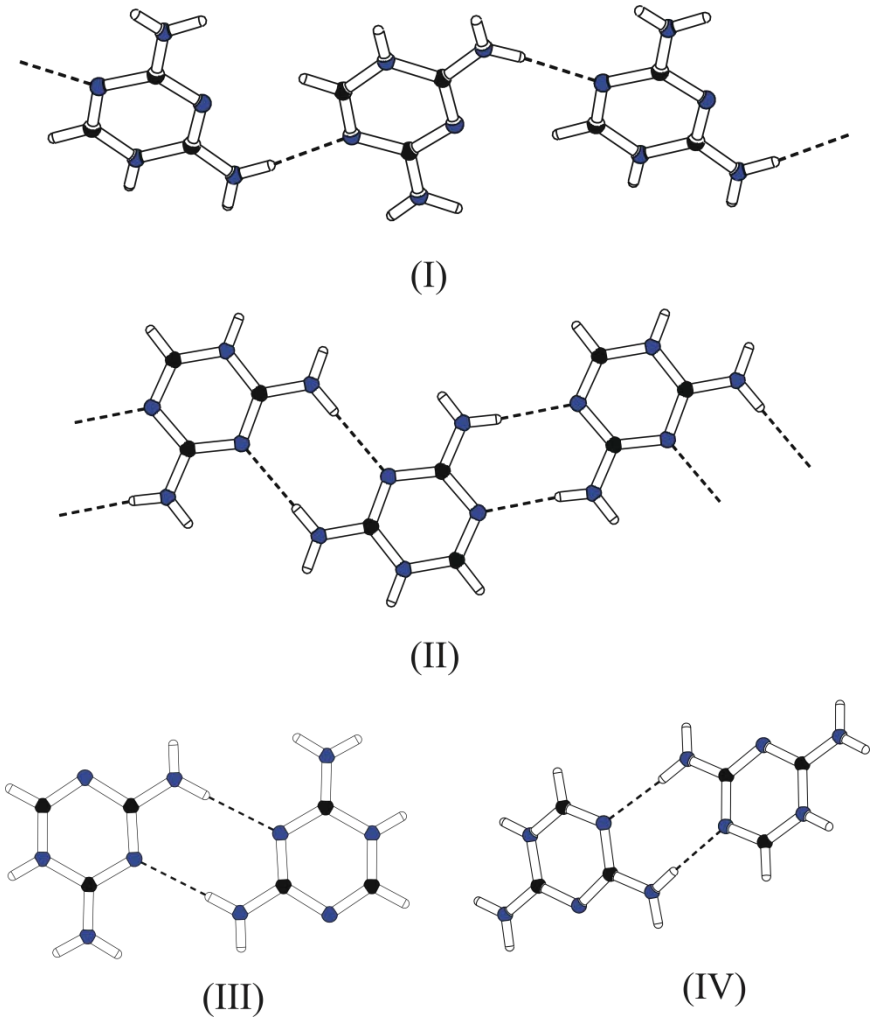

Figure 47: Types of arrangement of **DAMT** molecules or their cations.

Regarding to quantum – chemical calculations, bond length and angles were calculated and compared with the values read from determined crystal structures of obtained compounds. The results close fit together; nevertheless some differences are observed (*e.g.* bond length C1 – N10 or bond angle N10 – C3 – N11 in **DAMT(1+)** cation). This is because quantum – chemical calculations are performed for isolated molecule in vacuum and no hydrogen bonds are considered while actually the molecules interact together and they are interconnected *via* hydrogen bonds. The similar explanation can be provided for expected

vibrational frequencies in IR and Raman spectra in comparison to measured spectra. Although the calculated vibrational frequencies do not differ much from measured spectra, there are noticeable differences in peaks positions. It is also caused by not considering other molecule's influence and hydrogen bonding in quantum – chemical calculations. More sensitive than position of the peaks are even their intensities.

Three of these structures – **DAMT H_2glu**, **DAMT HLmal · H_2O** and **$(DAMT)_2$ Ltar** – exhibit non-centrosymmetric assembly so they were selected for examination of the second harmonic generation efficiency. For **DAMT H_2glu** also dependence of the intensity on the power of laser was measured. As seen in Figure 46 the intensity of SHG quadratically increases with the rising power of the laser.

8 Conclusion

This bachelor's thesis was focused on preparation and characterization of novel compounds suitable for NLO. In particular, the second harmonic generation (SHG) was the target property. The explored compounds were the crystalline salts and adducts of 2,4-diamino-1,3,5-triazine. In total, thirteen new salts were prepared and described. They were characterized mainly by using the methods of vibrational spectroscopy along with X-ray diffraction methods. For twelve of them crystal structures were determined. Besides that the quantum – chemical calculations were performed to predict the NLO properties and also for IR and Raman spectra assignment. Three of all prepared compounds exhibited non-centrosymmetric arrangement and that is why they were examined for the second harmonic generation efficiency in powdered samples. For the most promising compound – 2,4-diamino-1,3,5-triazinie – glutaric acid (1/1) (**DAMT H_2glu**) – also dependence of the SHG intensity on the power of laser was measured. The results reveal that 2,4-diamino-1,3,5-triazine is prospective base in the field of NLO in the form of cation as well as uncharged molecule.

9 References

(1) I. Matulková, I. Němec, P. Němec: *Československý časopis pro Fyziku*, **2011**, 61, 76 – 84.

(2) Ch. Bosshard, K. Sutter, Ph. Pretre, J. Hulliger, M. Florsheimer, P. Kz, P. Gunter: *Organic Nonlinear Optical Materials*, Overseas Publishers Association, Amsterdam **1995**.

(3) S. K. Park, J. Y. Do, J. J. Ju, S. Park, M. S. Kim, M. H. Lee: *Materials Letters*, **2005**, 59, 2872 – 2875.

(4) N. Bloembergem: *Nonlinear Optics*, http://www.coqus.at/fileadmin/quantum/coqus/documents/Bahaa_Saleh/CH21-Nonlinear-Optics.pdf (downloaded 13.8.2015)

(5) M. Fridrichová: *Disertační práce*, **2012**, Přírodovědecká fakulta UK v Praze, Praha.

(6) H. Nobutoki, H. Koezuka: *Journal of Physical Chemistry*, **1997**, 101, 3762 – 3768.

(7) S. R. Marder, J. W. Perry, C.P. Yakymyshyn: *Chemistry of Materials*, **1994**, 6, 1137 – 1147.

(8) K. Mohanalingam, M. Nethaji, P. K. Das: *Journal of Molecular Structure*, **1996**, 378, 177 – 188.

(9) D. Xue, S. Zhang: *Journal of Physical Chemistry*, **1997**, 101, 5547 – 5550.

(10) T. Pal, T. Kar: *Materials Chemistry and Physics*: **2005**, 91, 343 – 347.

(11) K. Aoki, K. Nagano, Y. Iitaka: *Acta Crystallographica*, **1971**, 27, 11 – 23.

(12) I. Matulková, I. Císařová, P. Němec, J. Kroupa, P. Vaněk, N. Tesařová, I. Němec: *Journal of Molecular Structure*, **2013**, 1044, 239 – 247.

(13) S. H. Park, K. Ogino, H. Sato: *Polymers for Advanced Technologies*, **2000**, 11, 349 – 358.

(14) P. Dastidar, T. N. G. Row, B. R. Prasad, C. K. Subramanian, S. Bhattacharya: *Journal of the Chemical Society – Perkin Transactions 2*, **1993**, 12, 2419 – 2422.

(15) M. Shyamala Devi, P. Tharmaraj, C. D. Sheela, R. Ebenzer: *Journal of Fluorescence*, **2013**, 23, 399 – 406.

(16) Y. Sui, Y. G. Liu, J. Yin, J. Gao, Z. K. Zhu, D. Y. Huang, Z. G. Wang: *Journal of Polymer Science*, **1999**, 37, 4330 – 4336.

(17) Y. Wang, C. U. Pittman, Jr., S. Saebo: *Journal of Organic Chemistry*, **1993**, 58, 3085 – 3090.

(18) G. Portalone: *Acta Crystallographica*, **2007**, 63, o3232 – o3232.

(19) *Omnic 8.3*, Thermo Nicolet, Corporation Madison, WI, USA.

(20) A. L. Spek: *Acta Crystallographica Section D*, **2009**, D65, 148 – 155.

(21) PANalytical B.V., *X'Pert HighScore* 2.2e **2009**.

(22) Gaussian, Inc., *Gaussian 09*, Revisio A.02, Wallingford CT, **2009**.

(23) R. Dennington, T. Keith, J. Millam, K. Eppinnett, W. L. Hovell, R. Gilliland: *GaussView*, Version 4.2.1, Semichem, Inc.Shawnee Mission **2006**.

(24) K. Nakamoto: *Infrared and Raman Spectra of Inorganic and Coordination Compounds, Part A: Theory and Applications in Inorganic Chemistry*, Fifth Edition, John Wiley and Sons, Inc., New York, Chichester, Weinheim, Brisbane, Singapore, Toronto **1997**.

(25) I. Matulková, J. Cihelka, M. Pojarová, K. Fejfarová, M. Dušek, P. Vaněk, J. Kroupa, R. Krupková, J. Fábry, I. Němec: *CrystEngComm*, **2012**, 14, 4625 – 4636.

(26) M. Fridrichová, I. Němec, I. Matulková, R. Gyepes, F. Borodavka, J. Kroupa, J. Hlinka, I. Gregora: *Vibrational Spectroscopy*, **2012**, 63, 485 – 491.

(27) G. Socrates: *Infrared and Raman Characteristic Group Frequencies*, Thirt Edition, John Wiley and Sons, LTD, Chichester, New York, Weinheim, Toronto, Brisbane, Singapore **2000**.

(28) I. Matulková, I. Němec, I. Cśařová, P. Němec, P. Vaněk: *Journal of Molecular Structure*, **2010**, 996, 23 – 32.